Surface Chemistry of Chloroiodomethane, Coadsorbed with H and O, on Pt(111)

X.-L. Zhou,† Z.-M. Liu, J. Kiss,‡ D. W. Sloan, and J. M. White*

Contribution from the Department of Chemistry and Biochemistry, University of Texas at Austin, Austin, Texas 78712

Received June 22, 1994®

Abstract: Using temperature programmed desorption (TPD), predosed oxygen TPD (POTPD), high-resolution electron energy loss spectroscopy (HREELS), and Auger electron and X-ray photoelectron spectroscopy (AES and XPS), we have investigated the chemistry of chloroiodomethane ($ClCH_2I$) dosed onto clean, D-covered and O-covered Pt(111). At or below 100 K, $ClCH_2I$ adsorbs molecularly on all these surfaces. While $ClCH_2I$ in physisorbed multilayers desorbs reversibly, a significant portion in the first monolayer dissociates during heating. In the absence of D and O, dissociation begins with C−I bond cleavage at ~150 K. Once the C−I bond breaks, several competitive reactions take place below 260 K: (1) hydrogenation of $CH_2Cl(a)$ to form $CH_3Cl(g)$ beginning near 150 K, (2) $Cl-CH_2(a)$ bond cleavage to form Cl(a) and $CH_2(a)$ above 170 K, (3) dehydrogenation of $CH_2(a)$ to CH(a) beginning near 180 K and increasing rapidly above 200 K, (4) hydrogenation of $CH_2(a)$ to $CH_4(g)$ above 170 K, and (5) HCl and H_2 formation and desorption above 200 K. At 260 K, the surface species are identified as I(a), CH(a), Cl(a), and a small quantity (~0.02 ML) of $CH_2(a)$. The remaining $CH_2(a)$ reacts with itself and Cl(a) to form $CH_4(g)$, HCl(g), and CH(a) at 360 K. Cl(a) remnants react with CH(a) at 415 K, producing HCl(g) and CCH(a). The residual CH(a) fragments react at 520 K, yielding $H_2(g)$, $C_x(a)$, and more CCH(a). Finally, dehydrogenation of CCH(a) occurs between 550 and 700 K, releasing H_2 and leaving carbon, presumably clustered. Coadsorbed D atoms weaken the bonding between $ClCH_2I$ and the surface, decrease the amount of $ClCH_2I$ dissociating, and suppress the complete decomposition to carbon for those $ClCH_2I$ molecules that do dissociate. In TPD with coadsorbed D, besides the addition products (i.e., CH_3D, CH_2D_2 and CH_2DCl), there are also H−D exchange products for methane (i.e., CHD_3 and CD_4) but not for methyl chloride (i.e., no CHD_2Cl and CD_3Cl). Coadsorbed O atoms attenuate slightly the dissociation of $ClCH_2I$, but strengthen its bonding with the surface. With increasing O coverage, the yields of CH_4, CH_3Cl, H_2, and HCl (reaction products found in the absence of O(a)) decrease; other reaction productts, H_2O, CO_2, CO, CH_2O, and CH_2Cl_2, appear and increase. To our knowledge, this is the first report of formaldehyde produced by the oxidation of a CH_2 precursor on Pt(111). Reaction paths are discussed, as are the effects of coadsorbed halogen atoms on hydrogenation, C−C coupling, and oxidation of CH_2.

1. Introduction

The surface chemistry, including photochemistry, of halogenated hydrocarbons is receiving considerable attention for several reasons. First, these molecules serve as important precursors for preparing surface hydrocarbon intermediates.[1-7] Because carbon−halogen (C−X) bonds (except C−F) are typically weaker than C−H and C−C bonds and because they can be selectively dissociated through irradiation with photons or low energy electrons, these molecules are viable precursors to selected hydrocarbon fragments. Both thermal[1-6] and nonthermal[8-10] methods have been employed. The surface chemistry of these fragments, of great importance in hydrocarbon catalysis, can then be studied in a great detail. Second, halogenated hydrocarbons or halocarbons are well-known environmental pollutants,[11] and their fundamental chemistry on solid surfaces is relevant to environmental protection and cleanup technologies. Third, halogenated hydrocarbons are important agents for the processing of silicon-based electronic materials.[12,13]

We have studied the surface chemistry of chloroiodomethane ($ClCH_2I$) on Pt(111), with and without coadsorbed atomic hydrogen or oxygen. One motivation was to study the thermal activation of C−Cl bonds, which plays an important role in the catalytic destruction of halogenated hydrocarbons. For simple alkyl chlorides adsorbed on Pt(111), raising the surface temperature typically results in the desorption of parent molecules; the C−Cl bonds remain intact.[9,14,15] Because alkyl iodides

† Present address: Water Research Institute, Inc., 4949 W. Orem Dr., Houston, TX 77045.

‡ Reaction Kinetics Research Group of the Hungarian Academy of Science and Institute of Solid State and Radiochemistry, University of Szeged, P.O. Box 105, H-6701 Szeged, Hungary.

® Abstract published in *Advance ACS Abstracts*, March 1, 1995.

(1) Zaera, F. *Acc. Chem. Res.* **1992**, *25*, 260 and references therein.
(2) Chiang, C.-M.; Wentzlaff, T. H.; Bent, B. E. *J. Phys. Chem.* **1992**, *96*, 1836 and references therein.
(3) Solymosi, F.; Revesz, K. *Surf. Sci.* **1993**, *280*, 38.
(4) Solymosi, F.; Kovacs, I. *Surf. Sci.* **1993**, *280*, 171.
(5) Kovacs, I.; Solymosi, F. *J. Phys. Chem.* **1993**, *97*, 11056.
(6) Liu, Z.-M.; Zhou, X.-L.; Buchanan, D. A.; Kiss, J.; White, J. M. *J. Am. Chem. Soc.* **1992**, *114*, 2031.
(7) Colaiaznni, M. L.; Chen, P. J.; Gutleben, H.; Yates, J. T., Jr. *Chem. Phys. Lett.* **1992**, *191*, 561. Gutleben, H.; Lucas, S. R.; Cheng, C. C.; Choyke, W. J.; Yates, J. T., Jr. *Surf. Sci.* **1991**, *257*, 146.
(8) Zhou, X.-L.; Zhu, X.-Y.; White, J. M. *Surf. Sci. Rep.* **1991**, *13*, 73.
(9) Lloyd, K. G.; Roop, B.; Campion, A.; White, J. M. *Surf. Sci.* **1989**, *214*, 227; *Catal. Lett.* **1989**, *2*, 105.
(10) Zhou, X.-L.; Blass, P. M.; Koel, B. E.; White, J. M. *Surf. Sci.* **1992**, *271*, 427.
(11) Sittig, M. *Handbook of Toxic and Hazardous Chemicals and Carcinogens*; Noyes Publications: Park Ridge, NJ, 1985.
(12) Gentle, T. M.; Soukiassian, P.; Schuette, K. P.; Bakshi, M. H.; Hurych, Z. *Surf. Sci.* **1988**, *202*, L568.
(13) McFreely, F. R.; Yarmoff, J. A.; Taleb-Ibrahimi, A.; Beach, P. B. *Surf. Sci.* **1989**, *210*, 429. Roop, B.; Joyce, S.; Schultz, J.; Steinfeld, J. *J. Chem. Phys.* **1985**, *83*, 6012.
(14) Henderson, M. A.; Mitchell, G. E.; White, J. M. *Surf. Sci.* **1987**, *184*, L325. We note that this reference concludes that multilayers do not accumulate on Pt(111). Other work demonstrates that multilayer desorption peaks at 110 K on Pt(111).[15b]

0002-7863/95/1517-3565$09.00/0

decompose thermally on Pt(111) at low temperatures and because the C−I bond energy (56 kcal/mol) is much lower than the C−Cl bond (84 kcal/mol), thermal dissociation of $ClCH_2$−I may generate stable surface $ClCH_2$. In such fragments, the dissociation of C−Cl is typically competitive with C−H and C−C cleavage;[15-19] thus, study of thermal dissociation of C−Cl bonds becomes possible by first generating the Cl-containing hydrocarbon fragments. We find, as expected, that dissociation of adsorbed $ClCH_2I$ begins with C−I bond cleavage commencing at 150 K. The dissociation of the C−Cl bonds in the resulting $ClCH_2$ fragments starts at 170 K and is kinetically competitive with hydrogenation of $ClCH_2$.

A second motivation was to study the surface chemistry of methylene (CH_2) on Pt(111) using $ClCH_2I$ as a precursor. CH_2 is an important intermediate in Fischer−Tropsch synthesis and catalytic conversion of hydrocarbons.[20] While the chemistry of methyl (CH_3) fragments on Pt(111), derived from thermal and nonthermal dissociation of methyl halides and other CH_3-bearing molecules, has been extensively studied,[14,21-26] less is known about the surface chemistry of CH_2.[27,28] Berlowitz et al.,[28] using TPD, studied diazomethane (CH_2N_2) on Pt(111), with and without coadsorbed hydrogen or oxygen. There was evidence that CH_2N_2 adsorbed dissociatively at 110 K, producing surface CH_2 and gaseous N_2. In thermal desorption, H_2, CH_4, and C_2H_4 were observed with or without coadsorbed H. On O-covered Pt(111), CO, CO_2, and H_2O were observed in TPD. For CH_2CO, ketene, on Pt(111),[27] one of the proposed reaction pathways is dissociation to form transient CH_2 fragments that decompose to CH and H, hydrogenate to CH_4 and react with undissociated CH_2CO to form C_2H_4. These methylenes do not accumulate to concentrations observable to HREELS.

The chemistry of CH_2 on other metal surfaces has been reported. On Ag(111), CH_2, derived from thermal dissociation of adsorbed $ClCH_2I$, recombines exclusively to form C_2H_4.[19] On Cu(110), the same conclusion was reached using CH_2I_2.[2,29] On Pd(100), CH_2, derived from CH_2I_2, reacts to form CH_4 and C_2H_4.[4] For CH_2I_2 on Al, CH_2 radicals and C_2H_4 were found in TPD.[30] On polycrystalline Co and Ni, adsorbed CH_2Cl_2 dissociates at ~180 K to form CH_2 which decomposes in steps to CH and C at elevated temperatures.[31] In the diazirine−Pd(110) system, surface CH_2, formed at ~140 K, reacts at ~200 K, yielding gaseous CH_4 and C_2H_4.[32] On Ru(001), HREELS data indicates that adsorption of diazomethane at 80 K gives surface CH_2 which rearranges upon heating to 280 K, to a mixture of CH, CH_2, and CH_3. This mixture decomposes to C and H upon heating to 500 K.[33] For CH_2CO on Ru(001),[34] a fraction of adsorbed CH_2CO dissociates to CH_2 which reacts, presumably via C_2H_4, to form CCH_3(a), ethylidyne. CH_2 has also been identified in several other systems.[7,35-38]

In this study, we observe chemistry, in the presence of coadsorbed I and Cl, of CH_2 on Pt(111). Compared to CH_2N_2 on Pt(111),[28] there are both similarities and differences which are related to the presence of halogens. The primary reaction of CH_2 on Pt(111) is dehydrogenation to form adsorbed methylidyne, CH(a), and coincidental hydrogenation to gaseous methane, CH_4(g). This occurs at a much lower temperature, ca. 210 K, than for CH_3(a), ca. 280 K.[14,23] The coupling of CH_2(a) to form C_2H_4 found on other metal surfaces, e.g., Ag(111),[19] Cu(110),[2,29] Al,[30] Pd(110),[32] and Pd(100),[4] was not observed in this study; it has, however, been reported for CH_2N_2 on Pt(111).[28] In the presence of coadsorbed D, methane formation is enhanced and there is a H-for-D exchange reaction involving C−H bonds. In the presence of coadsorbed O, besides H_2O, CO and CO_2, formaldehyde (H_2CO) is produced during TPD. In addition, there is a new reaction channel—chlorination to form CH_2Cl_2, which does not occur in the absence of O.

2. Experimental Section

The experiments were carried out in two separate ultrahigh-vacuum chambers; both had a base pressure of (3−7) × 10^{-10} Torr. One (machine I) was equipped with temperature programmed desorption (TPD), Auger electron spectroscopy (AES), and Fourier transform mass spectroscopy (FTMS) (not used in this study) facilities and has been described elsewhere.[39] The second chamber (machine II) had high-resolution electron energy loss spectroscopy (HREELS), X-ray photoelectron spectroscopy (XPS), and TPD facilities; a more detailed description has been given previously.[40] The TPD and AES data presented in this paper were obtained from machine I and the HREELS and XPS data from machine II.

The Pt(111) crystal was cleaned by sequences of Ar ion sputtering at 300 K, oxidation at 800 K, and annealing at 1150 K; cleanliness was confirmed by AES or XPS. The crystal was cooled to 100 K, or slightly below, with liquid nitrogen and was heated resistively at a rate of 6 K/s for TPD (line-of-sight). The substrate temperature was monitored with a chromel-alumel thermocouple spot-welded to the back of the crystal. To prevent electrons, emitted from the QMS filament, away from the surface during line-of-sight TPD,[10] a stainless steel foil with a ~1.5 cm^2 square hole, covered with 80% transparent mesh, was placed on, but electrically isolated from, the head of the QMS. With the foil floated electrically, no current was measured between the Pt(111) and ground.

(15) (a) Jo, S. K.; White, J. M. *Surf. Sci.* **1991**, *245*, 305. (b) Jo, S. K.; White, J. M. *J. Am. Chem. Soc.* **1993**, *115*, 6934.
(16) Liu, Z.-M.; Zhou, X.-L.; Kiss, J.; White, J. M. *Surf. Sci.* **1993**, *286*, 233.
(17) Castro, M. E.; Pressley, L. A.; Kiss, J.; Pylant, E. D.; Jo, S. K.; Zhou, X.-L.; White, J. M. *J. Phys. Chem.* **1993**, *97*, 8476.
(18) Kadodwala, M.; Jones, R. G. *J. Vac. Sci. Technol.* **1993**, *A11*, 2019.
(19) Zhou, X.-L.; White, J. M. *J. Phys. Chem.* **1991**, *95*, 5575.
(20) Biloen, P.; Sachtler, W. M. H. *Adv. Catal.* **1981**, *30*, 165.
(21) Fairbrother, D. H.; Peng, X. D.; Viswanathan, R.; Stair, P. C.; M. Trenary, M.; Fan, J. *Surf. Sci. Lett.* **1993**, *285*, L455.
(22) Liu, Z.-M.; Zhou, X.-L.; White, J. M. *Appl. Surf. Sci.* **1992**, *52*, 249.
(23) Zaera, F.; Hoffmann, H. *J. Phys. Chem.* **1991**, *95*, 6297. Zaera, F. *Langmuir* **1991**, *7*, 1998.
(24) Henderson, M. A.; Mitchell, G. E.; White, J. M. *Surf. Sci.* **1991**, *248*, 279.
(25) Zaera, F. *Surf. Sci.* **1992**, *262*, 335; *Catal. Lett.* **1991**, *11*, 95.
(26) Berlowitz, P.; Yang, B. L.; Butt, J. B.; Kung, H. H. *Surf. Sci.* **1986**, *171*, 69.
(27) Radloff, P. L.; Mitchell, G. E.; Greenlief, C. M.; White, J. M.; Mims, C. A. *Surf. Sci.* **1987**, *183*, 377; Mitchell, G. E.; Radloff, P. L.; Greenlief, C. M.; Henderson, M. A.; White, J. M. *Surf. Sci.* **1987**, *183*, 403.
(28) Berlowitz, P.; Yang, B. L.; Butt, J. B.; Kung, H. H. *Surf. Sci.* **1985**, *159*, 540.
(29) Chiang, C.-M.; Wentzlaff, T. H.; Jenks, C. J.; Bent, B. E. *J. Vac. Sci. Technol.* **1992**, *A10*, 2185.
(30) Modl, A.; Domen, K.; Chuang, T. J. *Chem. Phys. Lett.* **1989**, *154*, 187. Domen, K.; Chuang, T. J. *J. Am. Chem. Soc.* **1987**, *109*, 5288.
(31) Steinbach, F.; Kiss, J.; Krall, R. *Surf. Sci.* **1985**, *157*, 401.
(32) Serghini Monim, S.; McBreen, P. H. *Surf. Sci.* **1992**, *264*, 341; *Chem. Phys. Lett.* **1992**, *192*, 547; *J. Phys. Chem.* **1992**, *96*, 2701. McBreen, P. H.; Serghini Monim, S.; Ayyoob, M. *J. Am. Chem. Soc.* **1992**, *114*, 2391.
(33) George, P. M.; Avery, N. R.; Weinberg, W. H.; Tebbe, F. N. *J. Am. Chem. Soc.* **1983**, *105*, 1393.
(34) Henderson, M. A.; Radloff, P. L.; White, J. M.; Mims, C. A. *J. Phys. Chem.* **1988**, *92*, 4111. Henderson, M. A.; Radloff, P. L.; Greenlief, C. M.; White, J. M.; Mims, C. A. *J. Phys. Chem.* **1988**, *92*, 4120. Henderson, M. A.; Zhou, Y.; White, J. M.; Mims, C. A. *J. Phys. Chem.* **1989**, *93*, 3688.
(35) Serghini Monim, S.; Venus, D.; Roy, D.; McBreen, P. H. *J. Am. Chem. Soc.* **1989**, *111*, 4106. McBreen, P. H.; Erley, W.; Ibach, H. *Surf. Sci.* **1984**, *148*, 292.
(36) Tjandra, S.; Zaera, F. *J. Catal.* **1993**, *144*, 361.
(37) Loggenberg, P. M.; Carlton, L.; Copperthwaite, R. G.; Hutchings, G. J. *Surf. Sci.* **1987**, *184*, L339.
(38) Zhou, Y.; Henderson, M. A.; Feng, W. M.; White, J. M. *Surf. Sci.* **1989**, *224*, 386. Backx, C.; de Groot, C. P. M.; Biloen, P. *Surf. Sci.* **1980**, *104*, 300.
(39) Zhou, X.-L.; Sun, Z.-J.; White, J. M. *J. Vac. Sci. Technol.* **1993**, *A11*, 2110.
(40) Zhu, X.-Y.; White, J. M. *J. Chem. Phys.* **1991**, *94*, 1555.

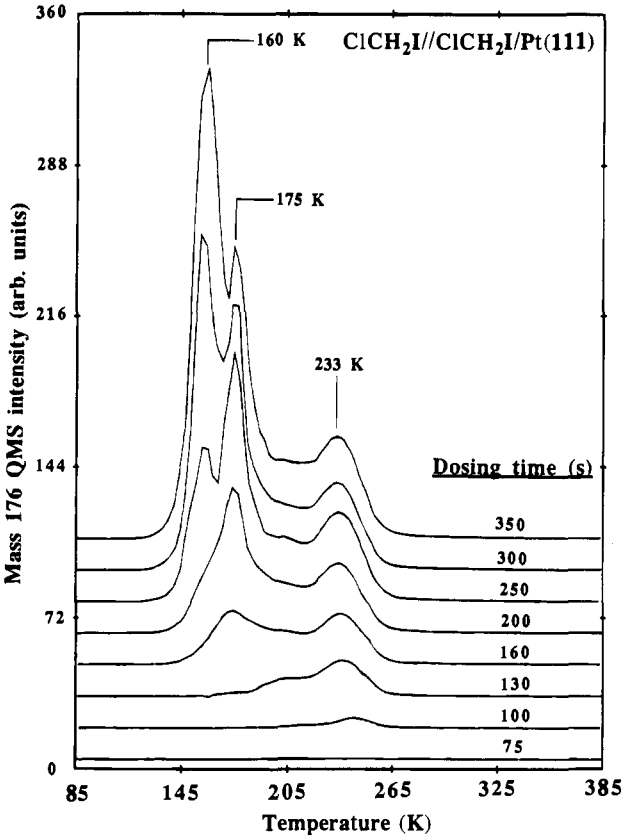

Figure 1. TPD spectra of molecular $ClCH_2I$ as a function of $ClCH_2I$ exposure on Pt(111) at 85 K. The exposures, expressed as dosing time (s), are indicated on each curve. To prepare for dosing, the ionization gauge current was incremented to a selected value by opening a leak valve to a source of $ClCH_2I$ (see section 2). The heating rate was 6 K/s.

$ClCH_2I$ (99% pure, Aldrich), a liquid at room temperature, was purified by several freeze–thaw–pump cycles under liquid nitrogen. Labeled oxygen, $^{18}O_2$ (99.1 at. % ^{18}O, Matheson), and D_2 (99.5%, Linde) were dosed, without further purification, through a tube which terminated approximately 7 mm away from the crystal. Dosing was initiated by turning the crystal to face the doser, having first opened a leak valve to increment the indicated ionization gauge pressure by 4 $\times$ 10^{-10} Torr. While this method gives very reproducible TPD results, the absolute exposures in Langmuirs (molecules cm^{-2}) are not known. Thus, relative exposures are given as dosing times.

XPS data were collected using 1253.6 eV Mg Kα X-rays and either 40 or 80 eV band-pass on the analyzer. HREELS spectra were taken with a primary electron energy of 3 eV and a typical resolution (FWHM) of 8 meV. Both the incident and detection angles were 60° with respect to the surface normal, i.e., specular scattering.

3. Results

3.1. $ClCH_2I$ on Clean Pt(111). 3.1.1. TPD and AES. For $ClCH_2I$ adsorbed on clean Pt(111) at 85 K, the subsequent TPD products were H_2, CH_4, HCl, CH_3Cl, I, and parent $ClCH_2I$; C_2 and higher hydrocarbons were not detectable. AES spectra, recorded after heating the crystal to 1050 K, revealed only a small quantity of adsorbed C. A full description of TPD results is presented below.

Figure 1 shows the TPD spectra of $ClCH_2I$ for different exposures (dosing time in seconds is indicated on each curve). For exposures of 75 s or less, molecular $ClCH_2I$ desorption was undetectable, indicating irreversible adsorption. For exposures of 100 s or longer, the $ClCH_2I$ TPD has peaks at 233 and at 175 K, both of which intensify and saturate at 250 s. Then, a third peak at 160 K appears. This low temperature peak grows continuously with increasing exposure and does not saturate, so we attribute it to a physisorbed multilayer. This agrees with our earlier result: multilayer $ClCH_2I$ adsorbed on Ag(111) desorbs at about 164 K.[19] The 233 K peak is attributed to $ClCH_2I$ molecules adsorbed in the first monolayer. We attribute the 175 K peak to adsorbed $ClCH_2I$ influenced by surface iodine. This is justified by the following facts. Heating the surface dosed with $ClCH_2I$ for 300 s at 85 to 700 K leaves 0.128 ML of atomic iodine and 0.102 ML of carbon on the surface (see below). We cooled this surface to 85 K, dosed $ClCH_2I$, and, in the subsequent TPD, found a much more intense $ClCH_2I$ peak at 175 K than in Figure 1. Evidence (see below) shows that cleavage of C–I bonds, forming I(a), starts at 150 K. The 175 K peak is certainly not due to the influence of surface carbon because there is no evidence for carbon formation below 180 K (see below). Figure 6, which summarizes peak areas as a function of exposure, shows that, for exposures longer than 200 s, the $ClCH_2I$ TPD area versus dosing time increases linearly, indicating a constant sticking coefficient and reversible adsorption of that $ClCH_2I$ which desorbs at 160 and 175 K. From Figure 1, we conclude that multilayers begin to form for doses exceeding 160 s.

Figure 2 shows the TPD spectra of one product, CH_3Cl. As for the parent, CH_3Cl was detected only for exposures exceeding 75 s. For 100 s dose, CH_3Cl has a peak at 216 K with a small shoulder at lower temperature. With increasing exposure, the peak intensifies and shifts down to 210 K. The shoulder also intensifies and, for exposures longer than 160 s, becomes an overlapping peak at about 190 K. After dosing CH_3Cl at 85 K, the monolayer and multilayer desorbed at 140 and 110 K, respectively, in agreement with earlier reports.[14,41] The desorption temperature of CH_3Cl in Figure 2 is much higher than 140 K, indicating that its desorption is reaction-limited. Based on the fact that, when $ClCH_2I$ is coadsorbed with D, CH_2DCl exceeds CH_3Cl in TPD (see section 3.2), we conclude that the formation of CH_3Cl involves hydrogenation of CH_2Cl. The CH_3Cl TPD peak appears at about 75 s and increases monotonically until it saturates at about 200 s. Saturation excludes the possibility that CH_3Cl is an impurity in the $ClCH_2I$.[41]

Figure 3 shows the CH_4 TPD spectra for the same experimental conditions as Figure 1. Methane first appears at 30 s—a small peak at 235 K. Two peaks at 220 and 270 K appear for a 50 s dose; at 75 s, the 270 K peak saturates and is buried under the tail of the 220 K peak; the latter continues to increase and saturates at 200 s. For exposures of 100 s and longer, there appear, in addition, a shoulder at about 200 K and a small peak at 355 K; both intensify and saturate at 200 s. As shown in Figure 6, the total CH_4 TPD area increases above 30 s and saturates at about 200 s.

The formation of CH_4 is attributed to dissociation of both C–I and C–Cl bonds and subsequent hydrogenation of the resulting CH_2 fragments. This is striking; C–Cl bonds in adsorbed CH_3Cl,[14] C_2H_5Cl,[9] and ClC_2H_4Br[15] on Pt(111) do not dissociate upon heating. On Ag(111), the Cl–C bond dissociates when $ClCH_2I$,[19] but not CH_3Cl[42] and C_2H_5Cl,[43] are dosed. Based on the known thermal behavior of alkyl halides on Pt(111) and the fact that C–I bonds are much weaker than C–Cl bonds (54 versus 80 kcal/mol), we propose that the dissociation of $ClCH_2I$ on Pt(111) begins with cleavage of C–I bond, consistent with XPS data (see section 3.1.2). Dissociation of C–Cl in the resulting CH_2Cl becomes competitive, compared

(41) Jo, S. K.; Zhu, X.-Y.; Lennon, D.; White, J. M. *Surf. Sci.* **1991**, *241*, 231.
(42) Zhou, X.-L.; Solymosi, F.; Blass, P. M.; Cannon, K. C.; White, J. M. *Surf. Sci.* **1989**, *219*, 294.
(43) Zhou, X.-L.; White, J. M. *Surf. Sci.* **1991**, *241*, 244.

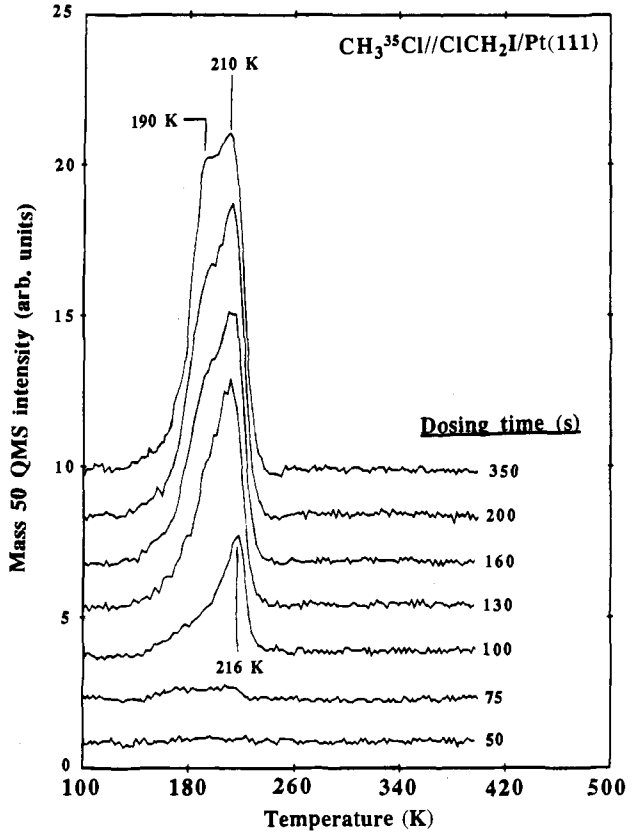

Figure 2. TPD spectra of CH_3Cl (monitored at $m/e = 50$) as a function of $ClCH_2I$ exposure on Pt(111) at 85 K. The 50 amu signal has been corrected for the cracking of $^{37}ClCH_2I$ at this mass. The experimental conditions were the same as Figure 1.

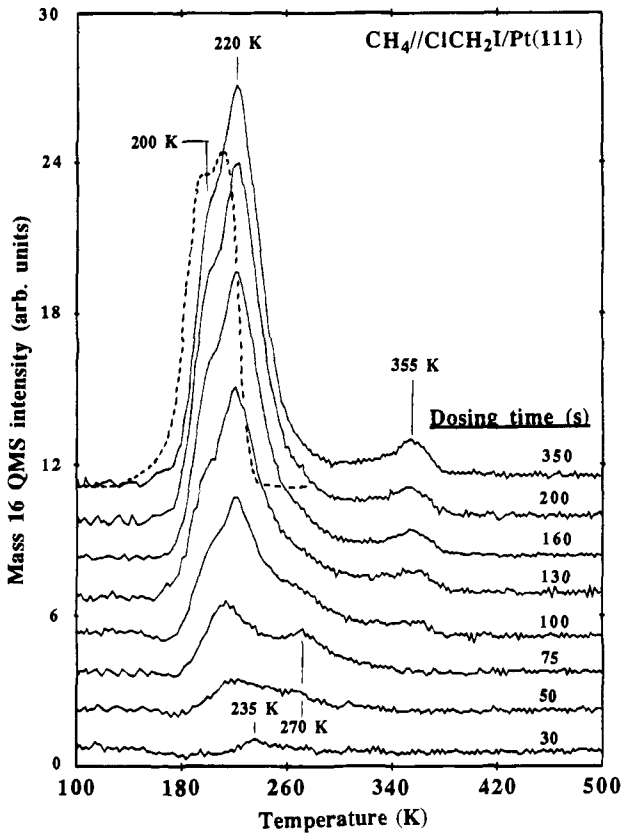

Figure 3. TPD spectra of CH_4 as a function of $ClCH_2I$ exposure on Pt(111) at 85 K. The experimental conditions were the same as Figure 1. The CH_3Cl spectrum (broken curve) is shown for comparison.

to C_2H_5Cl and CH_3Cl, because CH_2Cl is much more strongly bound to the substrate. For methyl and ethyl chloride, C−Cl cleavage cannot compete with parent desorption. In our case, the onset temperature of CH_4 desorption suggests that C−Cl dissociation commences at 170 K. While dissociation to CH_2(a) and Cl(a) is thermodynamically favored ($CH_2Cl(a) \rightarrow CH_2(a) + Cl(a)$, $\Delta H = -33$ kcal/mol on Pt(111),[44] some CH_2Cl is hydrogenated to form CH_3Cl. Clearly, H−CH_2Cl bond formation and CH_2−Cl bond dissociation compete kinetically between 170 and 220 K. On Ag(111), since there is no H(a) available, all CH_2Cl fragments dissociate, and the resulting CH_2 fragments recombine to form ethylene at 218 and 259 K.[19]

In two, partly repetitive panels with different vertical scales, Figure 4 shows the TPD spectra of HCl. Unlike the previous three TPD products, HCl grows in from the lowest exposures (Figure 6). At 10 s, i.e., about 5% of the exposure required to begin multilayer growth, the peak is 510 K; for longer doses, it intensifies and shifts to lower temperature, saturating at 130 s with a peak temperature of 415 K. At 20 s, a second peak, 315 K, emerges and shifts downward as the dose increases. There are two peaks, 240 and 265 K, for a 50 s exposure; we interpret the former as connected to the 315 K peak and the latter as arising from a different process. The low temperature peak becomes constant (220 K) for exposures longer than 75 s and its intensity saturates at 200 s. For 100 s, there is a new peak at 360 K; its position remains the same, but its intensity increases up to 200 s. The total HCl TPD area increases with $ClCH_2I$ exposure and, in common with other products, saturates at 200 s dose.

Clearly, HCl TPD is multifaceted. Wagner and Moylan[45] have recently studied the adsorption and desorption of HCl on Pt(111). At 90 K, it adsorbed dissociatively; recombination to form HCl dominated the TPD. At very low exposures, HCl desorbed as a single second order peak at about 400 K. At saturation, undissociated HCl desorbed as a major peak at 220 K and a shoulder at about 270 K. A small fraction of H(a) desorbed as H_2, leaving behind a small amount of Cl(a), which desorbed atomically at 960 K. In the presence of preadsorbed H(a), the fraction of Cl(a) which desorbed atomically decreased; the HCl peak at 220 K was still dominant, but the shoulder at 270 was attenuated, and the temperature at which HCl desorption ceased decreased from about 420 to 320 K. Comparing HCl desorption from $ClCH_2I$ with that from HCl, we find some similarities. The low temperature (<315 K) peak and shoulder in Figure 4 vary with exposure in almost the same ways as directly dosed HCl,[45] and, at saturation, both have a dominant peak at 220 K with a higher temperature shoulder.

For $ClCH_2I$, the desorption of HCl sets in at a higher temperature (185−190 K) than CH_4 (170 K), suggesting that C−Cl bonds begin to dissociate at 170 K, producing Cl(a). The latter starts to recombine with surface H atoms to produce gaseous HCl at slightly higher temperature. This is supported by the fact that, when $ClCH_2I$ is dosed with D_2, DCl dominates at 220 K (see section 3.2.1.). Especially for large doses, the H which is reacting, beginning about 180 K, comes mostly from C−H bonds. The amount of CH_4 and HCl desorbing is

(44) For $CH_2Cl(a) \rightarrow CH_2(a) + Cl(a)$ on Pt(111), we assume each Pt−C covalent bond worth 53 kcal/mol[74] and the Cl−Pt(111) bonding energy, D(Cl−Pt) is the same as the desorption energy of atomic Cl. Assuming a first-order kinetics with a prefactor of 10^{13} s^{-1} for the desorption of atomic Cl from Pt(111), we estimate a desorption energy of 60 kcal/mol from its desorption peak temperature of ~950 K (Figure 16). The value of ΔH for the reaction is then equal to $-[D(Cl-Pt)(60) + 2D(Pt-C)(106) - D(C-Cl)(80) - D(Pt-C)(53)] = -33$ kcal/mol.

(45) Wagner, F. T.; Moylan, T. E. *Surf. Sci.* **1989**, *216*, 361.

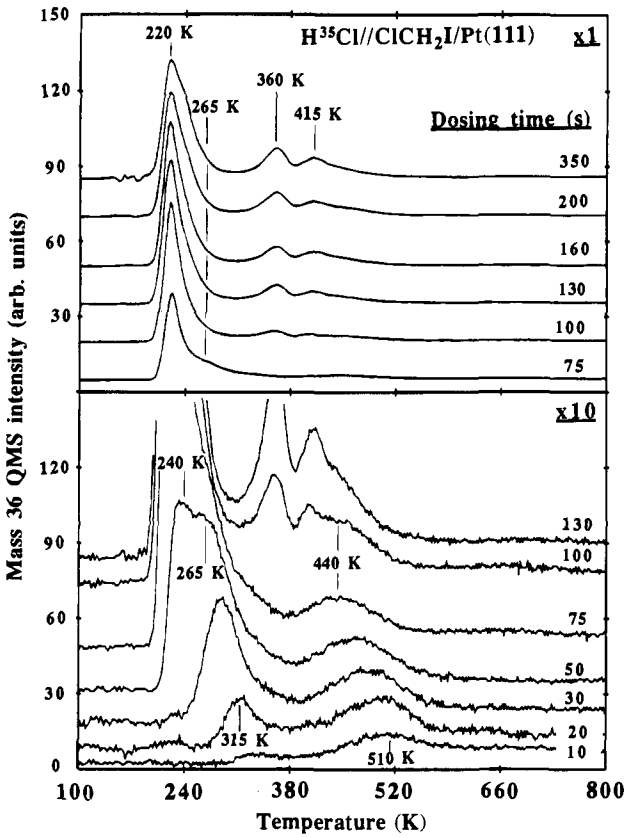

Figure 4. TPD spectra of HCl (monitored at m/e = 36) as a function of $ClCH_2I$ exposure on Pt(111) at 85 K. The experimental conditions were the same as Figure 1. Note the different vertical scaling factors of upper (×1) and lower (×10) panels.

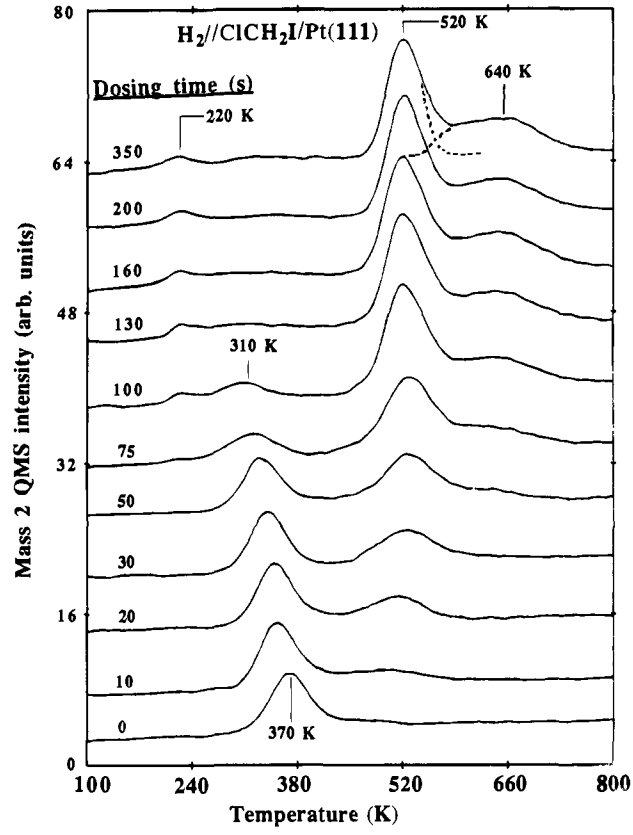

Figure 5. TPD spectra of H_2 as a function of $ClCH_2I$ exposure on Pt(111) at 85 K. The experimental conditions were the same as Figure 1. The curve labeled with zero (0) sec. shows desorption of H_2 due to adsorption of background H_2.

relatively large, so no more than a small fraction comes from background H_2 dissociative adsorption (see Figure 5). The high temperature (≥360 K) HCl peaks in Figure 4 were not observed when HCl was dosed.[45] XPS and HREELS (see below) show evidence that the kinetics are controlled by the dissociation of C−H bonds.

Figure 5 shows the H_2 TPD spectra. Without dosing $ClCH_2I$, there is a small H_2 peak at 370 K, which is due to dissociative adsorption of background H_2. Its peak area never exceeds 3% of that obtained by saturating the surface with H_2, and, as the $ClCH_2I$ exposure increases, its area decreases, disappearing for exposures ≥ 130 s. Even at the lowest doses, there is another H_2 TPD peak at 520 K. A broad H_2 peak at 640 K emerges at 50 s exposure. A small H_2 peak at 220 K becomes detectable at 75 s exposure; its intensity increases only slightly with $ClCH_2I$ exposure. According to Figure 6, the total H_2 TPD peak area saturates earlier (~100 s) than the other products (~200 s).

Unlike chlorine, iodine desorbs (not shown) atomically. In agreement with our earlier work,[6] this occurs at high temperatures, peaking between 850 and 925 K, depending on $ClCH_2I$ coverages. Compared to chlorine, atomic I is observed, in part, because C−I bonds are weaker than C−Cl, and H−I weaker than H−Cl. Therefore, for those adsorbed $ClCH_2I$ molecules that undergo C−I bond dissociation, some C−Cl bonds are preserved and CH_3Cl is released as a result of hydrogenation of CH_2Cl. While both H(a) + Cl(a) → HCl(g) (ΔH = 19 Kcal/mol) and H(a) + I(a) → HI(g) (ΔH = 44−49 Kcal/mol[46]) on Pt(111) are endothermic, in all likelihood, the former reaction is activated at much lower temperature, whereas activation of the latter is possible only when surface H is no longer available.

With some reasonable assumptions, we converted the TPD areas, as indicated on the ordinate of Figure 6, to absolute coverages in monolayers [one monolayer (ML) is defined as a surface adspecies/Pt ratio of unity]. Assuming, for dissociative H_2 adsorption on Pt(111) at 85 K, that the H/Pt surface ratio is unity when saturation is reached,[47] we can convert the H_2 TPD area from $ClCH_2I$/Pt(111) to coverage in ML. When the chemisorbed peak area for parent desorption (175 and 233 K) saturates, we calculate that 0.095 ML H(a) desorbs (as H_2). For $ClCH_2I$ exposures shorter than 30 s, H_2, HCl, and I are the only desorption products, i.e., each adsorbed $ClCH_2I$ molecule decomposes and produces one H atom (or 0.5 H_2 molecules), one HCl molecule, and one I atom. The initial linear increase in H_2 TPD area (Figure 6) thus yields a $ClCH_2I$ accumulation of 8.0×10^{-4} ML/s. Stoichiometrically, the initial linear increases in HCl and I TPD areas also correspond to 8.0×10^{-4} ML/s. Assuming that the sticking coefficient of $ClCH_2I$ at 85 K is constant, independent of coverage, we calculate, based on the measured TPD areas of HCl and I and their initial increases, that at saturation 0.128 ML $ClCH_2I$ decomposes and 0.109 ML HCl is produced. Since CH_3Cl is the only other Cl-containing species observed in TPD and no Cl atoms remain on the surface above 500 K, chlorine balance indicates that at saturation 0.019 ML CH_3Cl desorbs. Taking the H_2 adsorption from background (0.03 ML) into account and using hydrogen balance, we calculate that, at saturation, 0.007 ML CH_4 desorbs.

(46) The bonding energy is 62 kcal/mol for H−Pt(111),[74] 103 kcal/mol for HCl(g), and 71 kcal/mol for HI(g) [Weast, R. C. *CRC handbook of Chemistry and Physics*; CRC Press, Inc.: Boca Raton, FL, 1993)]. We estimate the bonding energy of 53−58 kcal/mol for I−Pt(111) from the desorption peak temperature (850−925 K) of atomic I and by assuming a first-order desorption kinetics with a prefactor of 1×10^{13} s^{-1}. ΔH for "H(a) + I(a) → HI(g)" on Pt(111) is then 44−49 kcal/mol. Since the Cl−Pt(111) bonding energy is 60 kcal/mol,[44] ΔH for "H(a) + Cl(a) → HCl(g)" on Pt(111) is then 19 kcal/mol.

(47) Weinberg, W. H. *Survey Prog. Chem.* **1983**, *10*, 1.

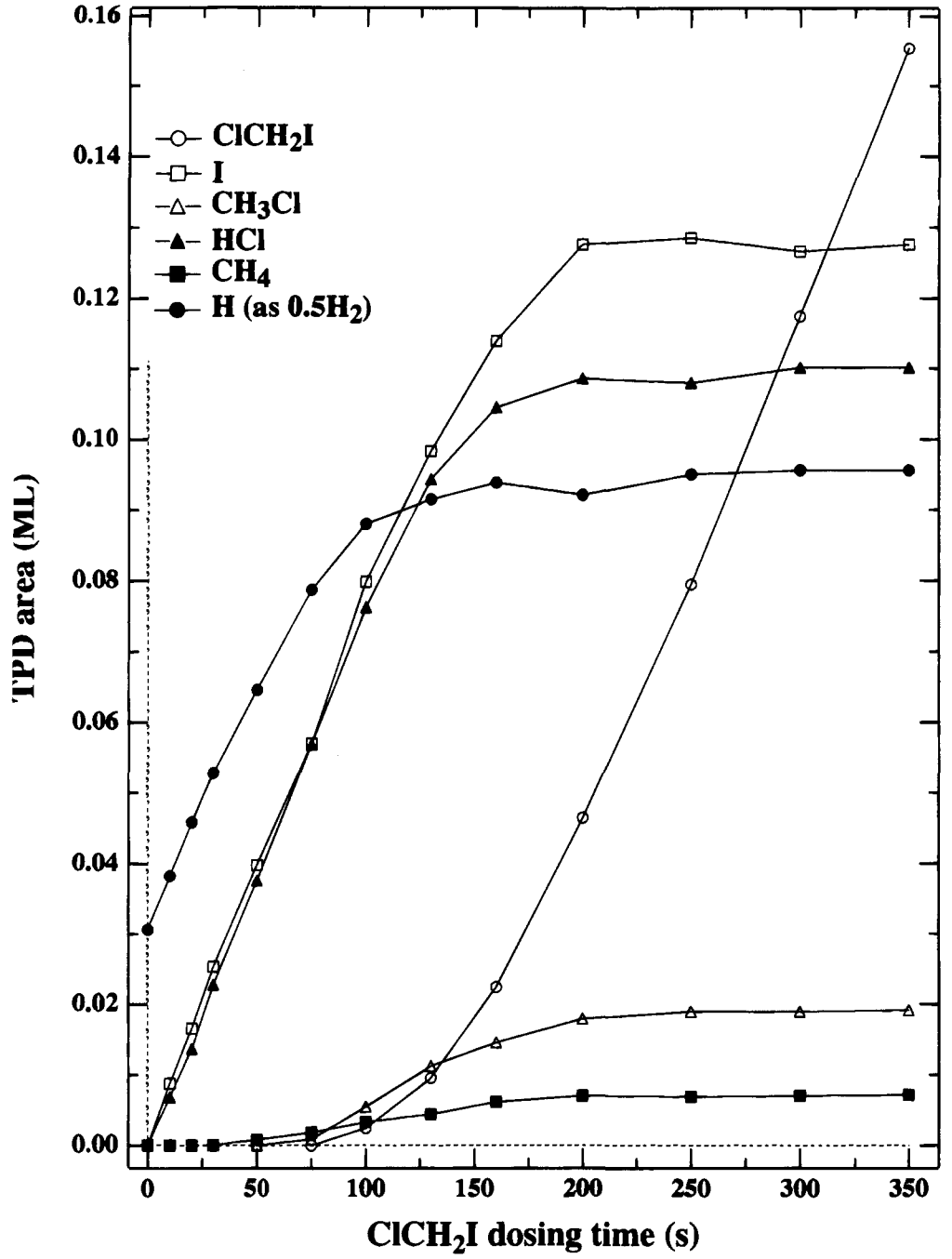

Figure 6. Summary of TPD areas for H (as 0.5 H_2), CH_4, HCl, CH_3Cl, I, and parent $ClCH_2I$ desorption as a function of $ClCH_2I$ dosing time (data from Figures 1–5).

Carbon balance indicates that at saturation 0.102 ML C is left on the surface. The saturation TPD area of H_2 desorbed at 520 and 650 K in Figure 5 corresponds to an H(a) coverage of 0.088 ML. This indicates that, after the desorption of CH_3Cl, CH_4, HCl, and $ClCH_2I$ has ceased and before the higher temperature (520 and 650 K) H_2 desorption commences (450 K), the surface carbon and hydrogen for a saturation $ClCH_2I$ dose correspond to a stoichiometry very near that of CH; HREELS (see below) confirms the presence of CH above 370 K.

These results indicate that, for those adsorbed $ClCH_2I$ molecules undergoing decomposition, complete decomposition to form gaseous H_2 and HCl and surface carbon is a major reaction channel (80%). The formation of CH_4 (5%) and CH_3Cl (15%) are minor channels. Compared to dosed CH_3I, the methane yield is much less (0.007 vs 0.08 ML), whereas the C yield is higher (0.102 vs 0.05 ML).[23] For $ClCH_2I$, the relatively weak C–Cl (~80 kcal/mol) bond, compared to C–H (~100 kcal/mol), provides Cl atoms which scavenge surface H atoms, resulting in a hydrogen-deficient situation and, consequently, low yields of CH_4 and CH_3Cl. When hydrogen is coadsorbed with $ClCH_2I$, the yields of CH_4 and CH_3Cl increase significantly (see section 3.2.).

3.1.2. XPS. To further characterize the dissociation process, the binding energies (BE) of I($3d_{5/2}$) and Cl(2p) as a function of annealing temperature for a single layer of $ClCH_2I$ were measured in machine II. The results for monolayer coverage are shown in Figure 7. Similar results were found for a surface dosed with multilayers of $ClCH_2I$, except for a dramatic drop of both I($3d_{5/2}$) and Cl(2p) intensities when the surface was heated to 170 K, a result of multilayer desorption (Figure 1).

At 100 K, XPS shows a symmetric I($3d_{5/2}$) peak at 620.4 eV and an asymmetric Cl(2p) peak at 199.9 eV (due to overlap of

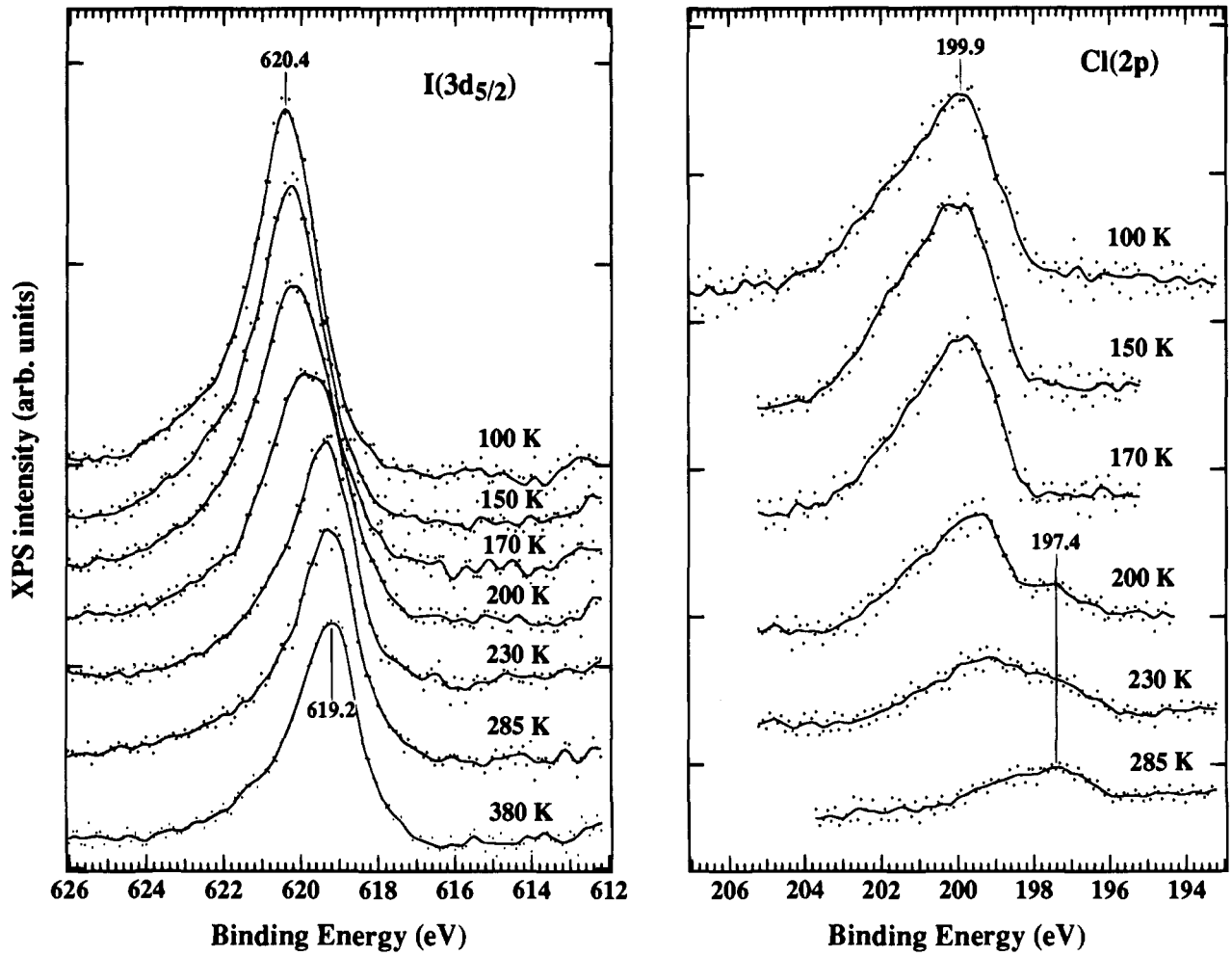

Figure 7. XPS spectra, taken at 100 K, of $I(3d_{5/2})$ and Cl(2p) for monolayer $ClCH_2I$ dosed on Pt(111) at 100 K and then heated to the indicated temperatures and recooled.

$Cl(2p_{1/2})$ and $Cl(2p_{3/2})$). This indicates that $ClCH_2I$ adsorption on Pt(111) at 100 K is mainly nondissociative; otherwise, multiple peaks for $I(3d_{5/2})$ and Cl(2p) would appear.[15,41,48] Upon annealing to any temperature below 150 K, neither $I(3d_{5/2})$ nor Cl(2p) XPS change. Between 150 and 230 K, both areas decrease, more for Cl(2p) than for $I(3d_{5/2})$, in harmony with TPD that shows desorption of CH_3Cl and HCl, besides $ClCH_2I$, in this temperature regime (Figures 1, 2, and 4). After heating to 170 K, there is a low BE $I(3d_{5/2})$ shoulder (619.2 eV) indicating formation of atomic iodine, I(a).[48] Peak synthesis indicates that 20% of the surface iodine is atomic, I(a), i.e., C−I bonds have broken. A careful comparison of the $I(3d_{5/2})$ spectra at 100 and 150 K indicates that a small number of C−I bonds dissociate even at 150 K. In contrast, the Cl(2p) position remains unchanged at 170 K. These important observations indicate that the C−I bond breaks first, consistent with TPD that shows a lower onset desorption temperature for CH_3Cl than for CH_4.

When the surface is heated to higher temperatures, the atomic I signal increases at the expense of the signal from the parent molecule. XPS indicates completion of C−I cleavage at 230 K; the $I(3d_{5/2})$ peak remains unchanged up to 700 K, i.e., constant area, symmetric, and positioned at 619.2 eV. At higher temperatures, I(a) desorbs. Based on TPD (0.13 ML $ClCH_2I$ dissociates) and a comparison of the $I(3d_{5/2})$ XPS areas at 170 and above 230 K, we calculate that only 0.05 ML of parent $ClCH_2I$ desorbs from a saturated first layer, i.e., dissociation dominates.

Turning to Cl(2p), a small peak appears at about 197.4 eV, indicating C−Cl bond cleavage and formation of Cl(1),[15,41] when the surface is heated to 200 K. Unlike $I(3d_{5/2})$, its intensity increases only slightly as the surface is heated to higher temperatures, even though the intensity at 199.9 eV, and, thus, the total Cl XPS signal, decreases. Cleavage of additional C−Cl bonds does occur above 200 K, but most of the resulting Cl(a) is promptly removed by reaction with H(a) to form HCl(g). After heating to 285 K, only the 197.4 eV peak remains. No Cl(a) was detected when the surface was heated to 500 K (not shown), consistent with TPD results that show no Cl-containing species desorbing above 500 K for large $ClCH_2I$ doses (Figure 4). The Cl(2p) XPS results indicate that HCl desorbing at 360 and 425 K (Figure 4) is from Cl(a) and confirm that its desorption is reaction-limited, i.e., the cleavage of C−H bonds in surface hydrocarbon fragments controls the HCl(g) formation rate. We note that H(a) does not accumulate above 300 K (see section 3.2.).

3.1.3. HREELS. Guided by TPD and XPS, we used HREELS to identify adsorbed species present at selected temperatures. Figure 8 shows spectra for monolayer and multilayer coverages of $ClCH_2I$ dosed at 100 K and spectra for various annealing temperatures (the annealing temperatures are indicated on each curve, and the spectra were taken after recooling). At 100 K, multilayer $ClCH_2I$ is characterized by

(48) Liu, Z.-M.; Akhter, S.; Roop, B.; White, J. M. *J. Am. Chem. Soc.* **1988**, *110*, 8708.

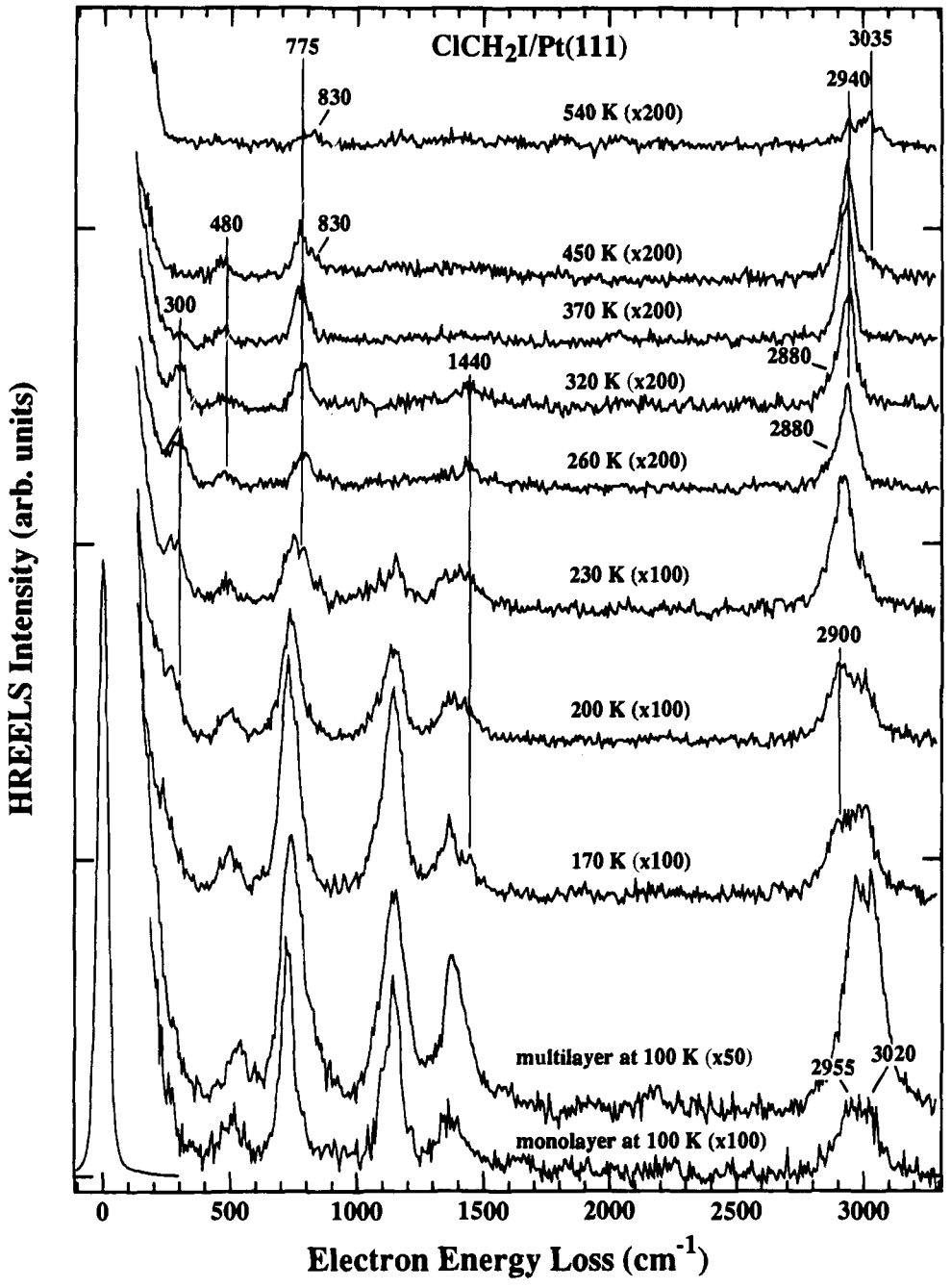

Figure 8. HREELS spectra for monolayer and multilayer doses of $ClCH_2I$ on Pt(111) at 100 K and for the multilayer warmed briefly to various temperatures as indicated. All the spectra were taken at 100 K.

losses at 540, 740, 820, 1150, 1380, 2970, and 3030 cm^{-1} and the monolayer at 500, 725, 1140, 1365, 2955, and 3020 cm^{-1}. The assignments, Table 1, match very closely those for liquid $ClCH_2I$,[49] confirming nondissociative adsorption of $ClCH_2I$ on Pt(111) at 100 K.

According to TPD and XPS, upon heating to 170 K the multilayer desorbs and some C−I bonds break. The HREELS confirms these processes; the spectrum shows losses at 500, 725, 1140, 1355, 1440, 2900, and 3020 cm^{-1}. The surface should contain both $CH_2Cl(a)$ and undissociated parent $ClCH_2I$. Therefore, while assigning the vibrations at 500, 725, 1140, 1355, and 3020 cm^{-1} to molecular $ClCH_2I$, we attribute the emerging losses at 1440 and 2900 cm^{-1} to $CH_2Cl(a)$. The loss at 1440 cm^{-1} is assigned to the scissor mode and that at 2900 cm^{-1} to the C−H stretching of CH_2 in $CH_2Cl(a)$. The latter is softened, compared to the parent, due to stronger coupling with the substrate. Similar observations have been made for CH_3I and CH_3 adsorbed on Pt(111):[14] the symmetric C−H stretching at 2970 cm^{-1} for $CH_3I(a)$ moves to 2925 cm^{-1} for $CH_3(a)$.

As expected, losses attributed to parent $ClCH_2I$ decrease when the surface is heated to 200 K, a result of molecular desorption and further dissociation. The latter leads to little change at 1440 and 2900 cm^{-1} because, during heating to 200 K, cleavage of additional C−I bonds is accompanied by hydrogenation and dissociation of $CH_2Cl(a)$ to form gas phase $CH_3Cl(g)$ and $CH_4(g)$ along with adsorbed $CH_2(a)$ and Cl(a). Any $CH_2(a)$ will contribute intensity to the 1440 and 2900 cm^{-1} loss regions. These gains and losses tend to compensate, resulting in little intensity change. A new loss, assigned to Pt−Cl stretching, emerges at 300 cm^{-1}.[9,45,50] Formation of Cl(a) at these temperatures is supported by the XPS data. Parenthetically, the

(49) Delwaulle, M. L.; Francois, F. *J. Phys. Radium Series* **1946**, *7*, 15.
(50) Grassian, V. H.; Pimentel, G. C. *J. Chem. Phys.* **1988**, *88*, 4478.

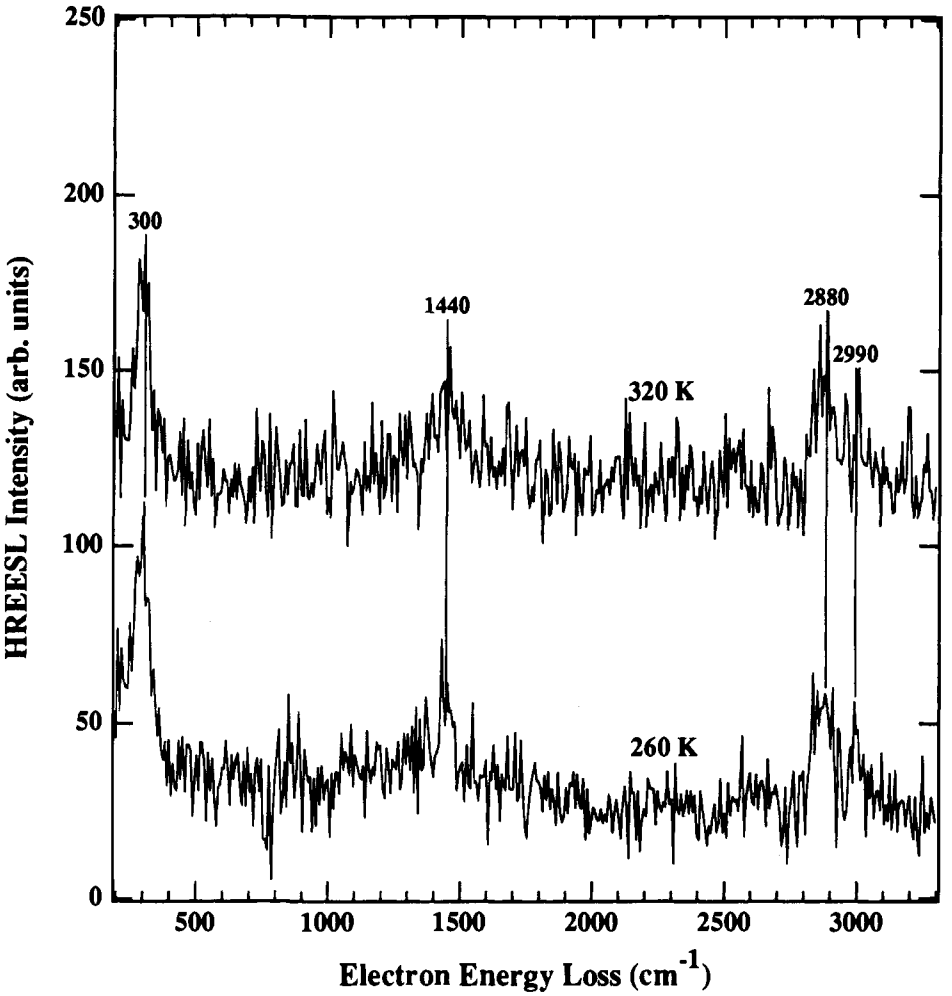

Figure 9. Difference HREELS spectra obtained by subtracting, in Figure 8, the 370 K spectrum from those at 260 and 320 K. See text for details.

Pt−I stretching frequency is probably too low to be resolved from the elastic peak.

Consistent with TPD and XPS, the HREELS spectra taken after heating to 230 and 260 K reflect removal of most and all the parent, respectively. At 260 K, the losses at 480, 775, and 2940 cm^{-1} are attributed to CH(a), i.e., Pt−C stretching, C−H bending, and C−H stretching, respectively. The peak at 1440 cm^{-1} and the shoulder at 2880 cm^{-1} are attributed to a small amount of CH_2(a) (see analysis below). No noticeable change in HREELS occurs when the surface is heated from 260 to 320 K, consistent with TPD that shows little desorption in this region.

When the surface is heated to 370 K, the Pt−Cl loss becomes significantly weaker, the 1440 cm^{-1} peak and the shoulder at 2880 cm^{-1} disappear. The losses attributed to CH(a) intensify slightly and the loss at 2940 cm^{-1} sharpens. These changes correlate with the TPD; HCl and a small amount of CH_4 desorb. We propose that, at 370 K, the surface retains CH(a), I(a), and a small quantity of Cl(a). The likely reactions at 355−360 K include $3CH_2(a) \rightarrow 2CH(a) + CH_4(g)$ and $CH_2(a) + Cl(a) \rightarrow CH(a) + HCl(g)$.

Heating to 450 K eliminates the Pt−Cl stretch, consistent with HCl desorption at 415 K. At the same time, CH(a) intensities decrease and new losses emerge at 830 and 3035 cm^{-1}. Between 450 and 540 K, CH(a) fragments dehydrogenate further, releasing H_2 at 520 K (Figure 5) and forming the species which give rise to the 830 and 3035 cm^{-1} signals. Tentatively, we assign them to η^2-CCH(a) (see below). They dominate after heating to 540 K but disappear by 800 K along with all other losses.

Before ending this section, we return to the losses at 1440 and 2880 cm^{-1}. As shown in Figure 8, after the surface is heated from 320 to 370 K, the HREELS peak in the C−H stretching region narrows and becomes symmetric and the loss at 1440 cm^{-1} disappears; the spectrum can be assigned to a single species, CH(a). To reduce the complexity of the spectra at 260 and 320 K, we subtracted, from each, a normalized version of the 370 K spectrum. The 775 cm^{-1} peaks were all normalized to unity, and the resulting spectra are shown in Figure 9. The difference spectra, though noisy, show three distinct peaks (300, 1440 and 2880 cm^{-1}). There may also be a peak at 2990 cm^{-1}. The 300 cm^{-1} peak is due to Pt−Cl stretching. The difference spectra are reasonably assigned to CH_2(a) with C_{2v} symmetry (Chart 1). Based on the dipole selection rule, we expect three loss modes. Symmetric C-H stretching (2880 cm^{-1}), CH_2 scissoring (1440 cm^{-1}), and Pt−C stretching (probably too weak to be observed). We will discuss this assignment in section 4.

3.1.4. POTPD. To monitor the cleavage of C−H bonds, we used predosed oxygen TPD (POTPD),[51] a thermal desorption and reaction technique based on scavenging H(a) by small amounts of preadsorbed O(a), formed from O_2. Provided the reaction temperature is above the normal water desorption temperature, the resulting water desorbs promptly and is easily detected. When hydrocarbon fragments dissociate and supply H, this water desorption monitors the C−H bond cleavage and, thus, characterizes the kinetics of dehydrogenation of hydrocarbon fragments on Pt(111).[51]

(51) Zhou, X.-L.; White, J. M. *J. Vac. Sci. Technol.* **1993**, *A11*, 2210.

Chart 1

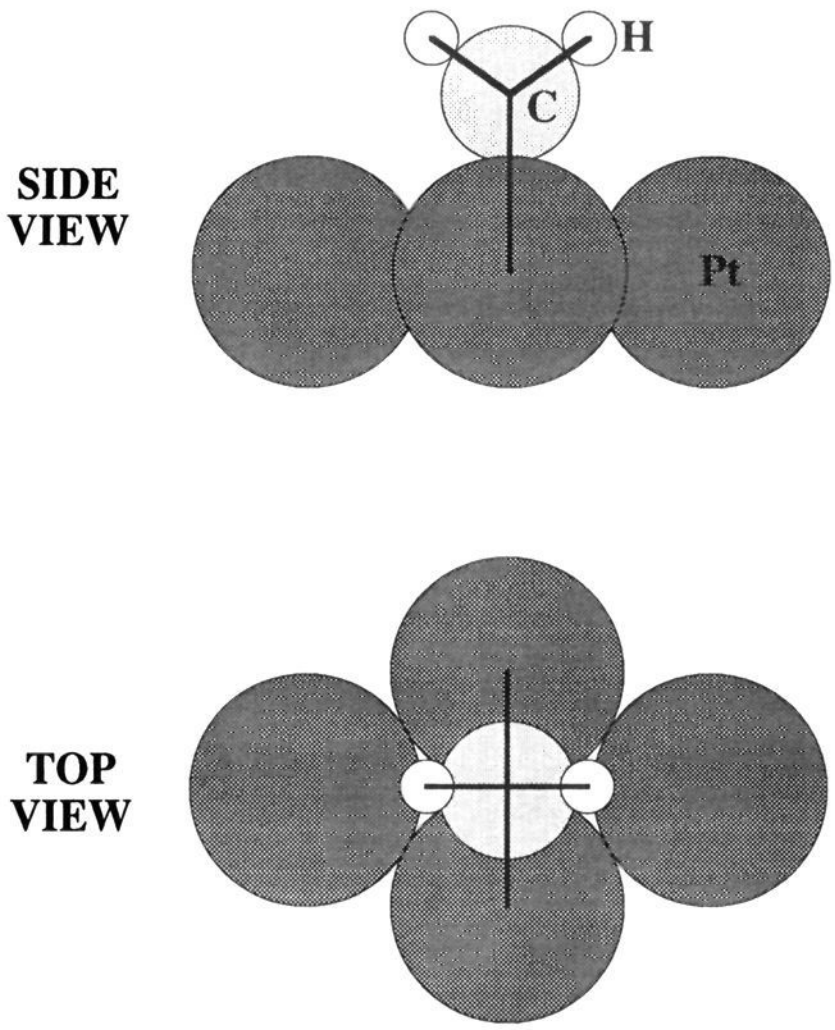

The upper panel in Figure 10 shows the H_2O TPD for a multilayer $ClCH_2I$ dosed on Pt(111) covered with 0.01 ML of O(a). Under these conditions, the only oxidation product is H_2O. Other products are distributed as when O(a) is absent, except that the TPD areas of H_2, CH_4, HCl, and CH_3Cl are slightly smaller. The H_2O TPD shows a peak at 215 K with an onset of about 170 K (dashed curve). To confirm that the H_2O desorption is rate-limited by the C−H bond cleavage, we exposed 0.01 ML ^{18}O, first to 0.3 L D_2 and then to $ClCH_2I$ for 300 s at 90 K. In this case, H_2O, HDO, and D_2O are all observed, and they have an onset of about 170 K (lower panel of Figure 10). However, the peak temperatures are measurably and reproducibly different—H_2O (215 K) > HDO (211 K) > D_2O (208 K). Above 208 K, as the D_2O desorption rate decreases due to the depletion of D(a), the rate of H supply, from the C−H bond dissociation, for forming H_2O continues to increase, resulting in the observed order. Since H(a) from the background contributes particularly in the low temperature portion of the H_2O TPD, the observed onset temperature for H_2O desorption is not a true measure of the onset for C−H bond dissociation. To account for this background effect, we took the following approximations. First, because isotope effects do not alter the *onset* temperature significantly, we neglected them in Figure 10. Under our experimental conditions, the D(a) coverage for a 0.3 L exposure of D_2 is 3.5 times the H(a) coverage adsorbed from background. Then, for the reaction of O(a) + 2H(a) [or 2D(a)] → H_2O(g) [or D_2O(g)], we subtracted the intensity of (D_2O + 0.5HDO)/3.5 from the dashed curve to eliminate the contribution of H_2O formed from background H(a) to the observed H_2O desorption intensity. The resulting spectrum (solid curve in the upper panel) shows a peak at 215 K with an onset of about 180 K, which we take as the onset of C−H bond dissociation. Thus, we conclude, consistent with the TPD of CH_4 and CH_3Cl, that C−H bond breaking sets in at 180 K and becomes quite rapid above 200 K. This is in agreement with the onset temperature of dehydrogenation of CD_2, derived from CD_2I_2, on Pt(111) where the effect of background hydrogen was eliminated.[51]

3.2. $ClCH_2I$ on D/Pt(111). To gain further insight, we examined cases in which both low and high coverages of atomic D were coadsorbed with slightly more than one layer of $ClCH_2I$ at 90 K. In TPD, we observed deuteration and H−D exchange products, i.e., *d*-labeled methyl chloride, hydrogen chloride, and methane.

Figure 11 compares the parent $ClCH_2I$ desorption with and without coadsorbed D. While the 157 (multilayer) and 176 K peaks remain unchanged when D is coadsorbed, the 233 K peak decreases and almost disappears when the coverage of D(a) is 0.5 ML. There is also a new parent peak (197 K at $\theta_D = 0.15$ ML), which intensifies and shifts to slightly lower temperature with increasing θ_D. Clearly, surface D lowers the desorption activation energy and reduces the dissociation of $ClCH_2I$. Comparing the amounts of atomic I that desorb, we calculate that 0.128, 0.12, 0.102, and 0.051 ML $ClCH_2I$ dissociates when 0.00, 0.15, 0.5, and 1.0 ML D(a), respectively, is present (Table 2).

Figure 12 shows the TPD spectra of hydrogen isotopes (panel A), methane (panel B), hydrogen chloride (panel C), and methyl chloride (panel D) for a multilayer $ClCH_2I$ coadsorbed with 0.15 ML D. For dihydrogen in the low temperature regime, there is a peak at 226 K for D_2, 230 K for HD, and 233 K for H_2. Desorption at these temperatures, the sharpness of the peaks, and the sequence D_2 < HD < H_2 are all consistent with desorption controlled by C−H cleavage, with an onset near 180 K, as for POTPD. In the high temperature regime, there are two peaks for H_2 and HD but no signal for D_2; HD peaks are *much weaker than* H_2. *These facts indicate some, but very little,* H−D exchange to form C−D bonds.

For methane (panel B), there is a peak at about 198 K for CH_4, CH_3D, CH_2D_2, CHD_3, and CD_4; CH_3D and CH_2D_2 are the strongest and both have onsets at about 170 K. Formation of CHD_3 and CD_4, requiring isotope exchange between D(a) and H in CH_2(a), is not surprising because exchange is kinetically facile on Pt(111).[25] There is also a peak at 226 K for CH_2D_2, a peak at 230 K for CH_3D, and a peak at 233 K for CH_4; the CH_3D peak is the most intense. For CH_4 and CH_3D there are relatively intense peaks at 355 K, but CH_2D_2 is barely detectable.

For hydrogen chloride (Figure 12C), DCl peaks at 220 K and HCl shows a strong peak at 225 K and two small peaks at 360 and 420 K. As in the absence of D(a), desorption of atomic Cl was not found. Compared to the clean surface (Figure 4), the high temperature peaks, 360 and 420 K, are much weaker when D is coadsorbed.

For methyl chloride (Figure 12D), there are two peaks, 190 and 220 K, for CH_3Cl and CH_2DCl but not for CHD_2Cl. It is interesting that no more than one D atom is incorporated into methyl chloride, while, in small amounts, fully deuterated methane (CD_4) is detected. This indicates that, unlike methane formation, no H−D exchange is involved in methyl chloride formation. We conclude that methyl chloride arises exclusively from the hydrogenation of CH_2Cl(a) and that its concentration drops to zero at about 240 K. It is also interesting that the CH_2DCl/CH_3Cl ratio is higher at 190 K than at 220 K. We understand this change as follows. At 190 K, the dehydrogenation is relatively slow, and the concentration of D exceeds H; thus, hydrogenation of CH_2Cl by D(a) dominates. At 220 K, dehydrogenation is rapid, much of the D is already consumed, and the resulting H atoms participate in hydrogenation of CH_2-Cl, increasing the relative CH_3Cl yield.

Figure 13 shows the TPD results for $ClCH_2I$ adsorbed on a higher coverage, 0.5 ML, of D(a). As expected, the relative concentration of D in the TPD products is higher than for θ_D =

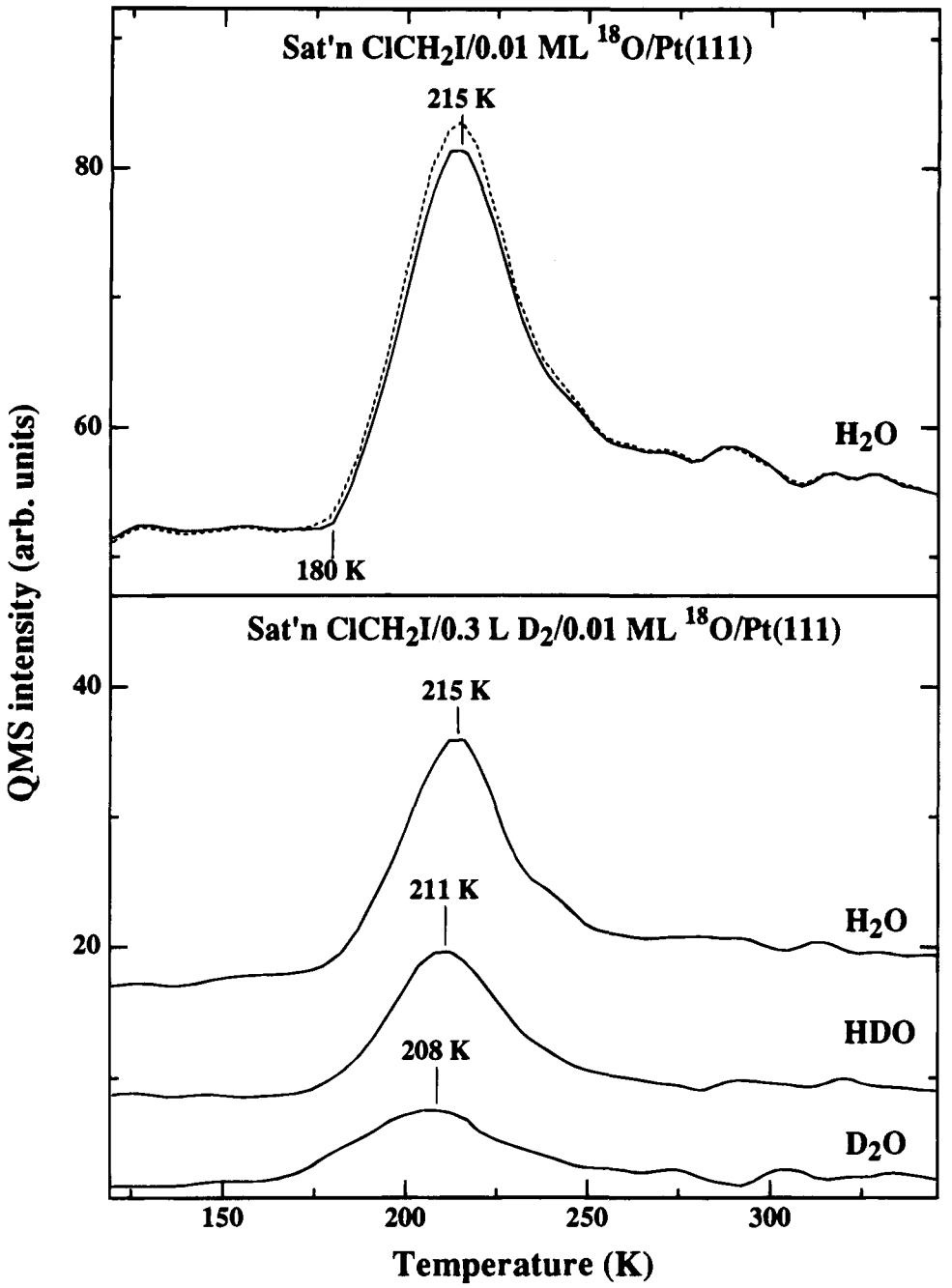

Figure 10. Upper panel: dashed curve—H_2O TPD spectrum for a multilayer coverage of $ClCH_2I$ dosed on 0.01 ML ^{18}O; solid curve—dashed curve minus the intensity of $[(D_2O + 0.5HDO)/3.5]$ from the lower panel (see text for details). Lower panel: H_2O, HDO, and D_2O TPD spectra for a multilayer coverage of $ClCH_2I$ on 0.01 ^{18}O predosed with 0.3 L D_2 at 90 K. The H_2O curve has been corrected for cracking of D_2O and HDO at 18 amu. The heating rate was 6 K/s.

0.15 ML. The lowest peak temperatures for dihydrogen desorption are slightly higher but have the same order, i.e., H_2 > HD > D_2 (Figure 13A). For methane (Figure 13B), there is no CH_4 peak at about 194 K and no peaks at 355 K. Instead, there is a new peak at 272 K for CH_4, CH_3D, and CH_2D_2. This is likely the result of hydrogenation of a methyl intermediate, CH_xD_{3-x}, because for $ClCH_2I$ coadsorbed with submonolayer CD_3I, there was a distinct peak at 275 K for CD_3H (not shown). For hydrogen chloride, there are no peaks at 360 and 420 K. For methyl chloride (Figure 13D), there are no qualitative differences compared to θ_D = 0.15 ML case.

The isotope distributions in methane, methyl chloride, and hydrogen chloride are summarized in Figures 14 and 15. For methane, the overall isotope distribution shifts to favor more D atoms in each molecule as θ_D increases. Although CHD_3 and CD_4 are detected for both low and high θ_D's, their yields are very low as compared to CH_3D and CH_2D_2, indicating that the isotope exchange between D and H in CH_2 is not strongly competitive with hydrogenation and dehydrogenation of CH_2. The relative yields of CHD_3 and CD_4, compared to total methane (see Table 2), increase with θ_D. The ratios of DCl/HCl and CH_2DCl/CH_3Cl increase monotonically with increasing θ_D (Figure 15).

The total yields of methane, methyl chloride, hydrogen chloride, and iodine in TPD and surface carbon as a function of θ_D are shown in Table 2. The iodine yield decreases monotonically with increasing θ_D. For those adsorbed $ClCH_2I$ molecules that dissociate, the fraction of complete dissociation to form surface carbon decreases monotonically from 80% on D-free surface to 27% on 1 ML D/Pt(111). Correspondingly,

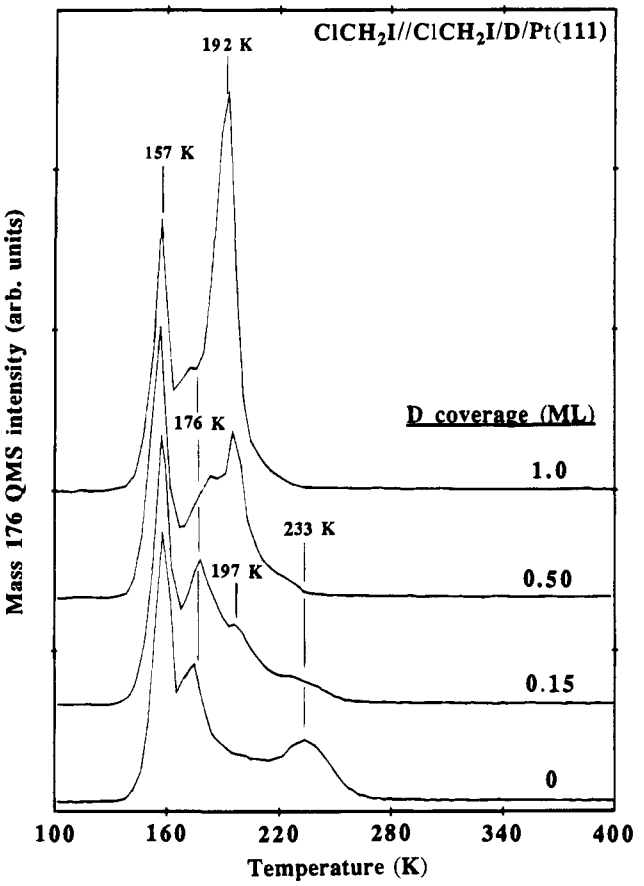

Figure 11. TPD spectra of $ClCH_2I$ for a multilayer exposure of $ClCH_2I$ on clean and D-covered Pt(111). The D coverage (ML) is indicated on each curve.

the relative yields of methane and methyl chloride increase monotonically with θ_D. All these indicate that coadsorbed D(a) blocks the dissociation of $ClCH_2I$, suppresses the dehydrogenation of CH_2, and enhances hydrogenation of CH_2Cl and CH_2.

We have also taken the $I(3d_{5/2})$ XPS, for coadsorbed $ClCH_2I$ and D, as a function of annealing temperature (results not shown). As on a D-free surface, the C—I bond starts to dissociate at 150 K, consistent with the onset temperature of CH_2DCl desorption. For the same exposure of $ClCH_2I$ and increasing θ_D, XPS indicates less and less atomic iodine after heating to 300 K, a result in agreement with the iodine TPD.

Even though D-for-H exchange reaction is detected in hydrogen and methane TPD, no C—D stretching signal was observed in HREELS between 100 and 700 K. A comparison of HD and H_2 TPD areas in Figure 12 and 13 indicates that the concentration of CD(a) is no more than 5% of that of CH(a) and probably lies below the detection limit of HREELS.

3.3. $ClCH_2I$ Coadsorbed with Atomic Oxygen. Because the oxidation of C_1 hydrocarbon fragments on metal surfaces is fundamentally related to the mechanism of catalytic oxidation of methane to form methanol, and because the catalytic oxidation of halogenated hydrocarbon wastes is environmentally interesting, we have also investigated the thermal reaction of $ClCH_2I$ with coverages of O(a) that exceed those used in POTPD. Figure 16 shows the TPD results for a multilayer dose of $ClCH_2I$ on 0.25 ML ^{18}O(a). For parent $ClCH_2I$, there is a new desorption peak at 305 K, in addition to the two other peaks that are found on O-free surfaces. Surface iodine desorbs atomically above 700 K with a peak at about 855 K. H_2 TPD is barely detectable. Methane and methyl chloride are still produced at 230 and 215 K, respectively, but their intensities are much lower than on an O-free surface. HCl shows several peaks—230, 270, 305, 350, and 460 K.

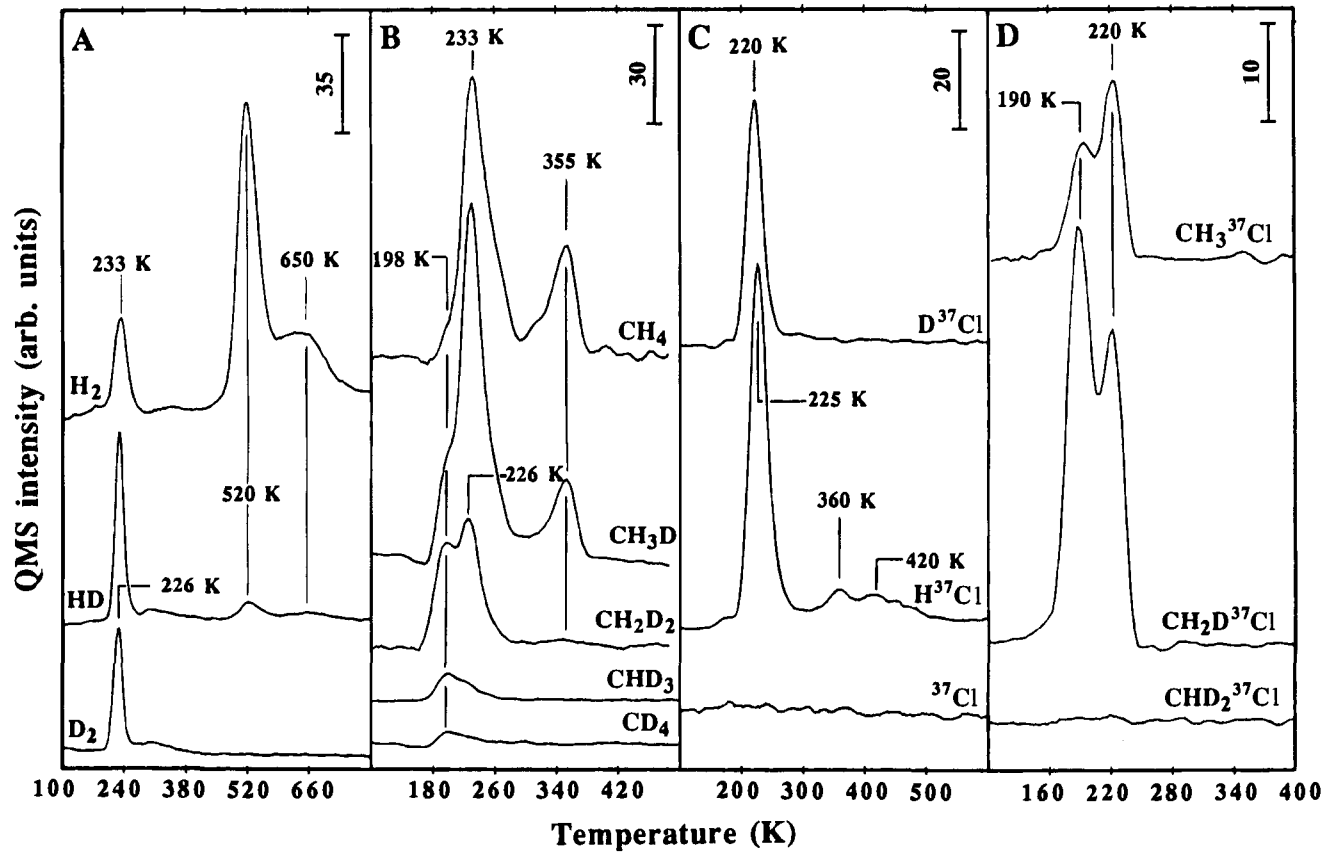

Figure 12. TPD spectra of dihydrogen (panel A), methane (panel B), hydrogen chloride (panel C), and methyl chloride (panel D) for a multilayer coverage of $ClCH_2I$ on 0.15 ML D.

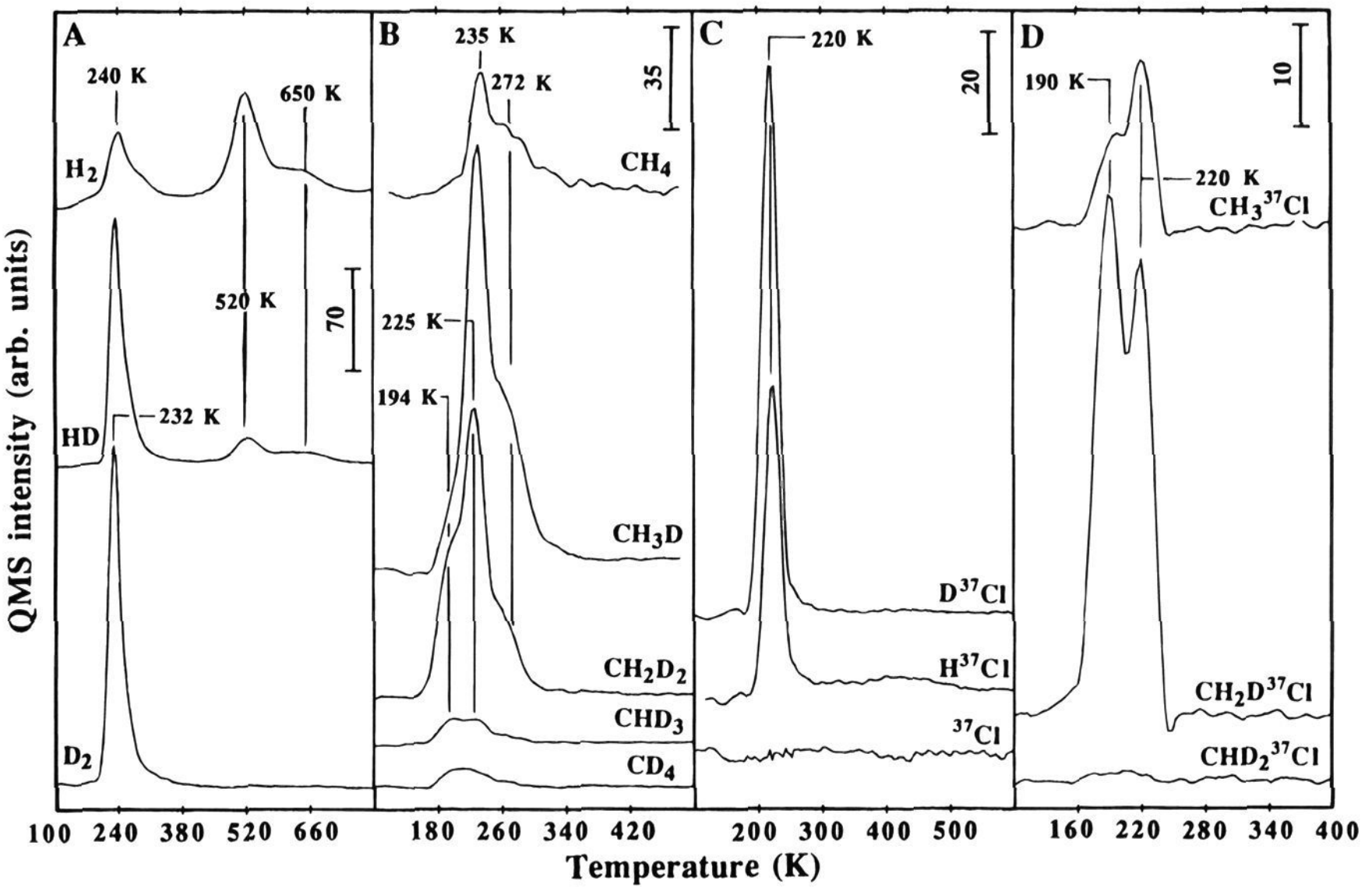

Figure 13. TPD spectra of dihydrogen (panel A), methane (panel B), hydrogen chloride (panel C), and methyl chloride (panel D) for a multilayer coverage of $ClCH_2I$ on 0.5 ML D.

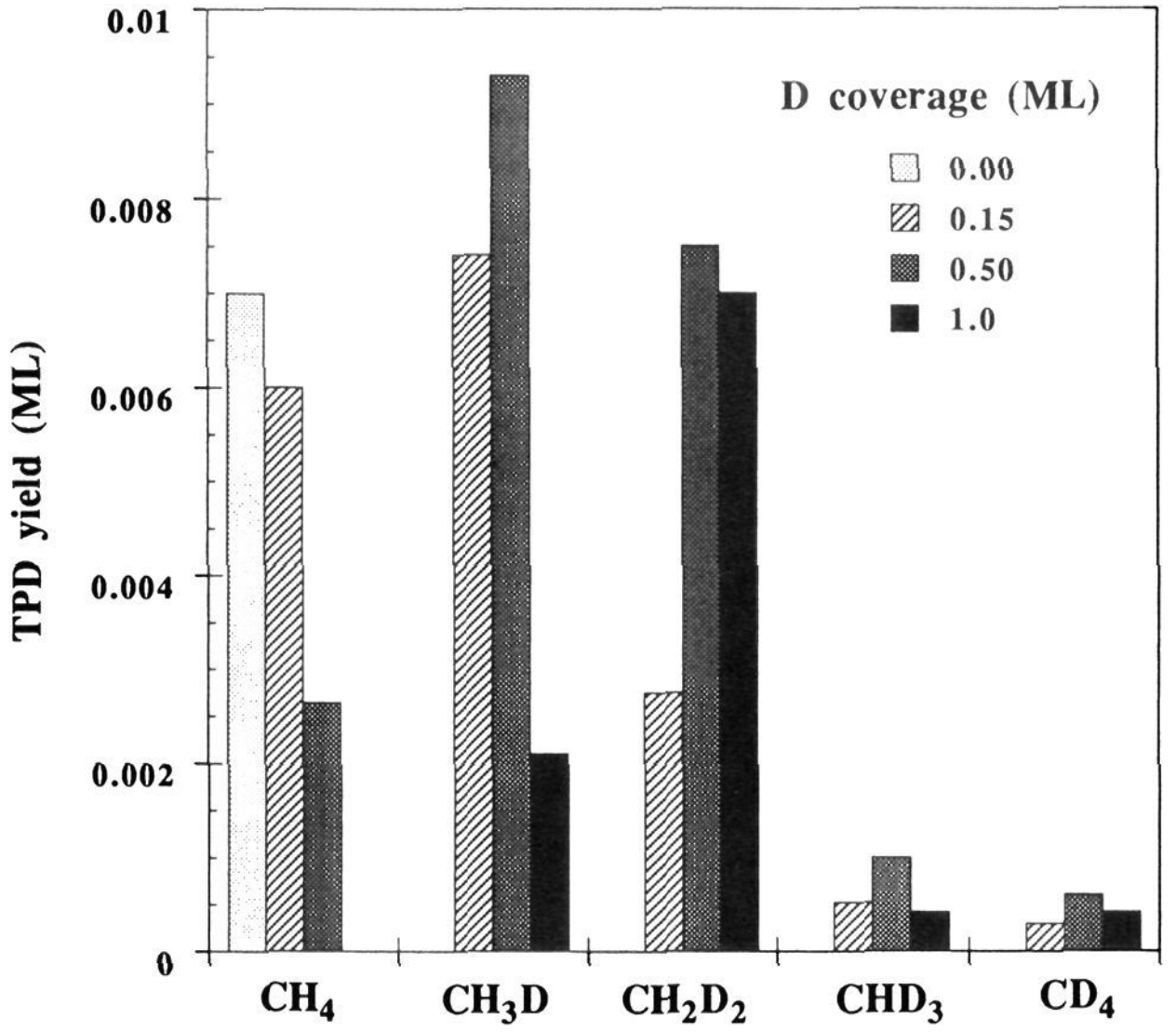

Figure 14. Isotope distributions in methane produced by heating a multilayer dose of $ClCH_2I$ over various amounts of D at 85 K.

Products not found on O-free surfaces are $H_2{}^{18}O$, $C^{18}O$, $CH_2{}^{18}O$ (formaldehyde), Cl, $C^{18}O_2$, and CH_2Cl_2. For the 30 amu ion signal, largely $C^{18}O^+$, contributions from the fragmentation of $C^{18}O_2$ and $CH_2{}^{18}O$ have been subtracted. And, for $C^{18}O_2$, the contribution of $CHCl^+$ (*m/e* = 48) from the fragmentation of $ClCH_2I$ and CH_2Cl_2 has been subtracted

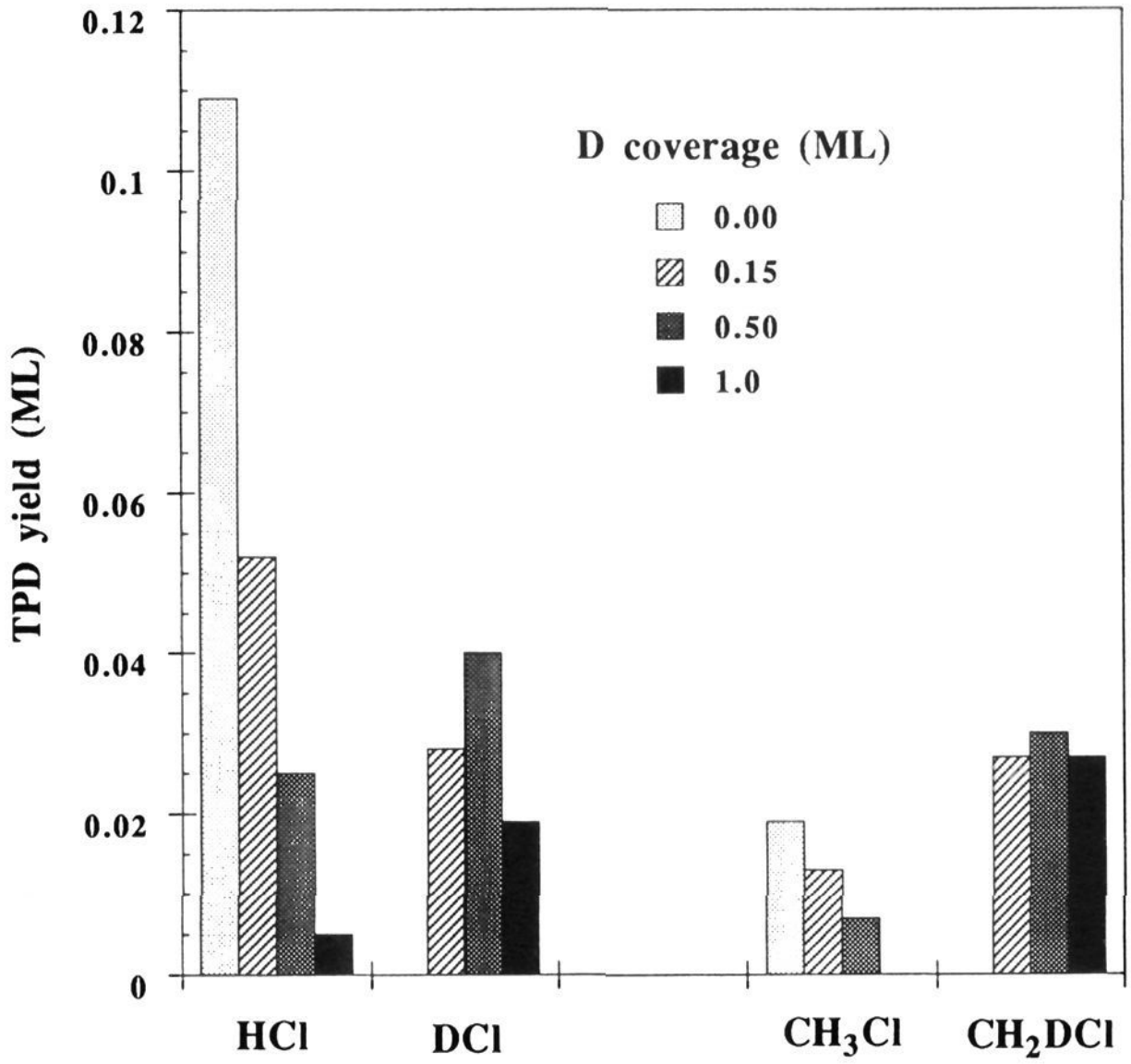

Figure 15. Isotope distributions in hydrogen chloride and methyl chloride produced by heating a multilayer dose of $ClCH_2I$ on Pt(111) partially covered with D.

Table 1. Assignments of Vibrational Spectra (cm^{-1}) of $ClCH_2I$[a]

mode	multilayer $ClCH_2I$/Pt(111)	monolayer $ClCH_2I$/Pt(111)	$ClCH_2I$[49]
$\nu_{as}(CH)$	3020	3030	3048
$\nu_s(CH)$	2955	2970	2979
$\delta_{as}(CH_2)$	1365	1380	1392
$\delta_s(CH_2)$	1140	1150	1183
$\varrho(CH_2)$	not resolved	820	801
$\nu(C-Cl)$	725	740	718
$\nu(C-I)$	500	540	527

[a] ν_{as}, asymmetric stretching; ν_s, symmetric stretching; δ, deformation or scission; ω, wagging; τ, twisting, ϱ, rocking.

Table 2. TPD Product Yields (ML) for Multilayer $ClCH_2I$ on D/Pt(111)

D coverage	methane	methyl chloride	hydrogen chloride	iodine	surface carbon
0.00	0.007	0.019	0.109	0.128	0.102
0.15	0.017	0.040	0.080	0.120	0.063
0.50	0.021	0.037	0.065	0.102	0.044
1.00	0.010	0.027	0.024	0.051	0.014

(note: hereafter, "^{18}O" will be replaced by "O"). There are four peaks, 225, 305, 360, and 410 K, for H_2O, one peak at 445 K for CO, three peaks, 305, 360, and 425 K, for CO_2, one peak at 305 K for CH_2Cl_2, and a peak at 280 K with a shoulder at about 175 K for CH_2O ($m/e = 32$). The assignment of $m/e = 32$ signal to CH_2O was confirmed by comparison of the measured TPD intensities of $m/e = 32$ (CH_2O), 31 (CHO) and 30 (CO) with the known fragmentation pattern of CH_2O. We searched for, but did not find, methanol (CH_3OH). This is in contrast to a similar experiment using CH_3I, where both formaldehyde and methanol are found.[52] To our knowledge, this is the first time, on Pt(111), that formaldehyde has been reported from the UHV reaction between a CH_2 precursor and atomic O, in the presence of coadsorbed halogens. Whereas in the absence of O(a), atomic Cl desorption is not observed, it clearly desorbs at about 950 K in the presence of O(a).[45] This can be easily understood; O(a) scavenges most H atoms to form H_2O, leaving insufficient H to form HCl. For the same reason, H_2 is not observed in TPD.

The detailed TPD results for a multilayer exposure of $ClCH_2I$, preadsorbed with different coverages of O(a), are shown in Figure 17, and the TPD areas of the reaction products versus θ_O are summarized in Figure 18. With increasing θ_O, all the hydrogenation products decrease, while Cl, CH_2Cl_2 and the oxidation products increase. Generally, these changes are the result of very effective consumption of H(a) by O(a). For parent $ClCH_2I$ (panel A), the peak intensity at 235 K decreases with increasing θ_O, but the high temperature cutoff increases. At $\theta_O = 0.12$ ML, there is a shoulder at 305 K which intensifies and becomes a distinct peak at $\theta_O \geq 0.19$ ML. For CH_4 (panel B), the shoulder at 200 K and small peak at 355 K found on O-free surfaces both disappear at $\theta_O = 0.035$ ML. For CH_3Cl (panel C), the intensity drops, but the shape and position change very little. For HCl (panel D), a new peak appears at 305 K for $\theta_O = 0.12$ ML, and its intensity increases with the coverage of oxygen. The highest temperature HCl peak (415 K) first intensifies and then diminishes with increasing θ_O; the peak temperature, however, increases monotonically to 460 K at $\theta_O = 0.25$ ML. All the H_2 peaks decrease with increasing θ_O (panel E).

We now turn to the products that increase with θ_O. The number and strength of the H_2O (panel 17 F) peaks varies with θ_O. One strong peak at 225 K sets in at low coverage,

(52) Zhou, X.-L.; White, J. M., manuscript to be published.

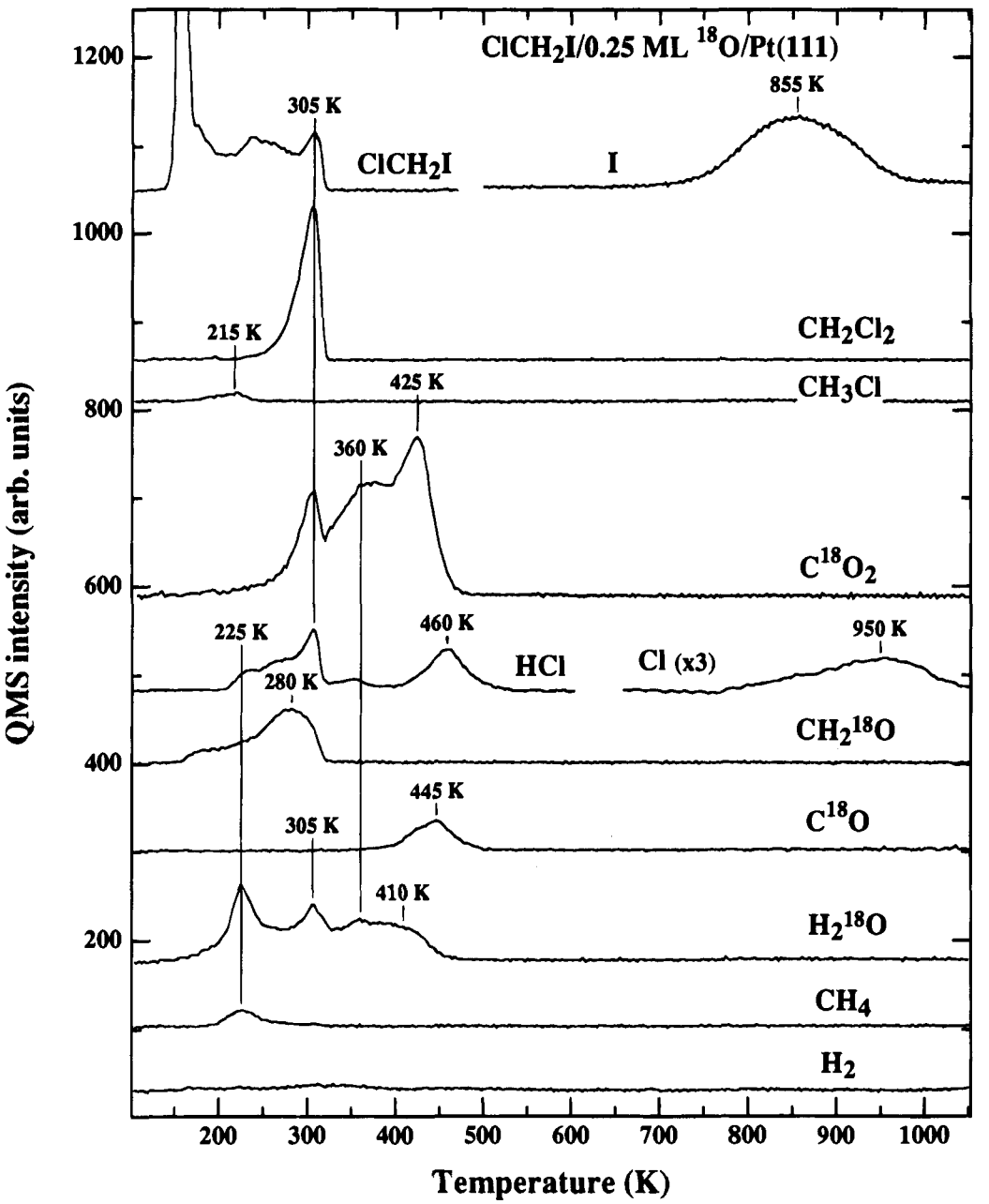

Figure 16. TPD spectra for multilayer $ClCH_2I$ dosed onto 0.25 ML ^{18}O at 85 K. The heating rate was 6 K/s.

maximizes (θ_O = 0.12 ML), and then decreases. Several higher temperature H_2O peaks, which we associate with dissociation processes that produce H(a), emerge at high θ_O—a 305 K appears at θ_O = 0.06 ML, a 350 K peak at θ_O = 0.035 ML, and a 380–410 K peak at θ_O = 0.12 ML. While the 350 K peak appears to approach saturation, the other two peaks increase monotonically. CH_2Cl_2 (panel G) is first detected at θ_O = 0.035 ML; it intensifies with increasing θ_O. CH_2O (panel H) is also first detected at θ_O = 0.035 ML. The lowest temperature peak at 175 K saturates at θ_O = 0.12 ML, while a second peak (280 K) emerges at θ_O = 0.06 ML and grows monotonically. Likewise, CO_2 (panel I) desorption is first detected at θ_O = 0.035 ML (peaks at 305 and 360 K). For $\theta_O \geq$ 0.19 ML, an additional peak at 425 K emerges. Ignoring background desorption peaked at 400 K, there is only one CO peak at 445 K (panel J); its area has a local maximum at θ_O = 0.12 ML.

As shown in Figure 18, the iodine TPD area decreases slowly with increasing θ_O; adding θ_O = 0.25 ML of O(a) reduces the dissociation by 20%.

XPS data were also taken in the presence of O(a) (Figure 19). Slightly more than one layer of $ClCH_2I$ was added to 0.25 ML O(a) at 100 K. The BEs, reflecting nondissociative adsorption, are 620.4 eV for I($3d_{5/2}$) and 199.9 eV for Cl(2p), just as on the O-free surface (Figure 7). Upon annealing briefly to 170 K, both I($3d_{5/2}$) and Cl(2p) weaken due to multilayer $ClCH_2I$ desorption. As the annealing temperature increases, the Cl(2p) peak position remains unchanged up to 210 K, while I($3d_{5/2}$) broadens slightly toward lower BE even at 170 K; as on the O-free surface, C–I bonds break more readily than C–Cl. Above 310 K, the I($3d_{5/2}$) spectra no longer change. Between 210 and 250 K, C–Cl cleavage is evidenced by growth of a peak at 197.3 eV. Its intensity does not increase much, if at all, at higher temperature; even though the surface concentration of Cl–C bonds drops dramatically, most of the Cl is carried off in desorbing products. Some 199.9 eV Cl(2p) signal remains at 290 K, but not at 320 K; i.e., C–Cl bonds are lost in this interval. The desorption of CH_2O, H_2O, and CH_4 (Figure 16) below 210 K indicates the availability of H(a) and CH_2(a). However, based on the absence of detectable XPS intensity at

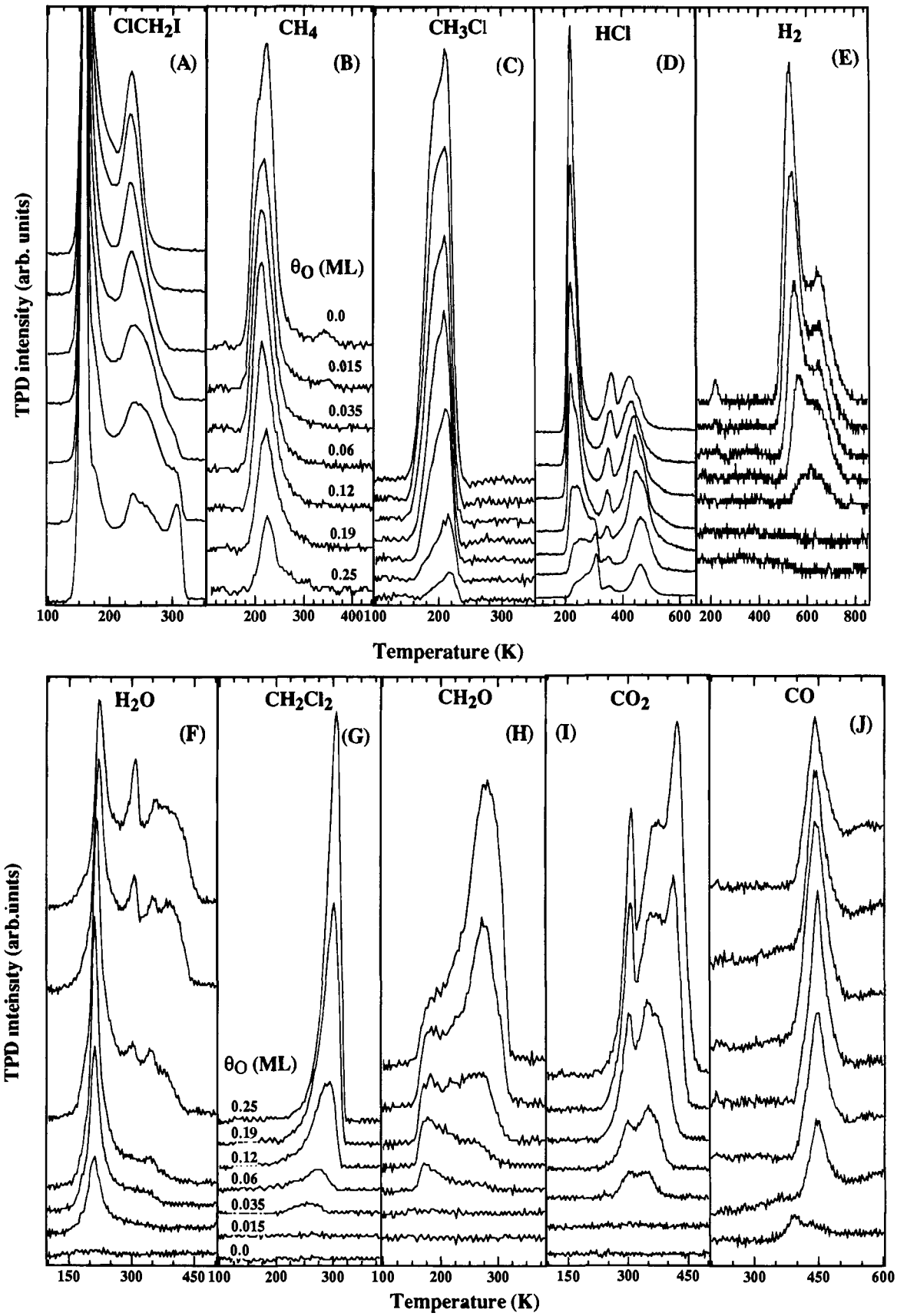

Figure 17. TPD spectra of $ClCH_2I$ (A), CH_4 (B), CH_3Cl (C), HCl (D), H_2 (F), $H_2{}^{18}O$ (G), CH_2Cl_2 (H), $CH_2{}^{18}O$ (I), $C^{18}O_2$ (J), and $C^{18}O$ (K) for multilayer $ClCH_2I$ coadsorbed with various amounts of atomic oxygen, ^{18}O—0, 0.015, 0.035, 0.06, 0.12, 0.19, and 0.25 ML—on Pt(111) at 85 K. The heating rate was 6 K/s.

197.3 eV, the dissociation of C—Cl to form Cl(a) is slow below 210 K (see HREELS data below).

Figure 20 shows the HREELS results for about two layers of $ClCH_2I$ adsorbed on 0.25 ML O(a) at 100 K and then heated to different temperatures. For O alone on Pt(111), HREELS shows a peak at 460 cm^{-1}, corresponding to Pt-O stretching, in

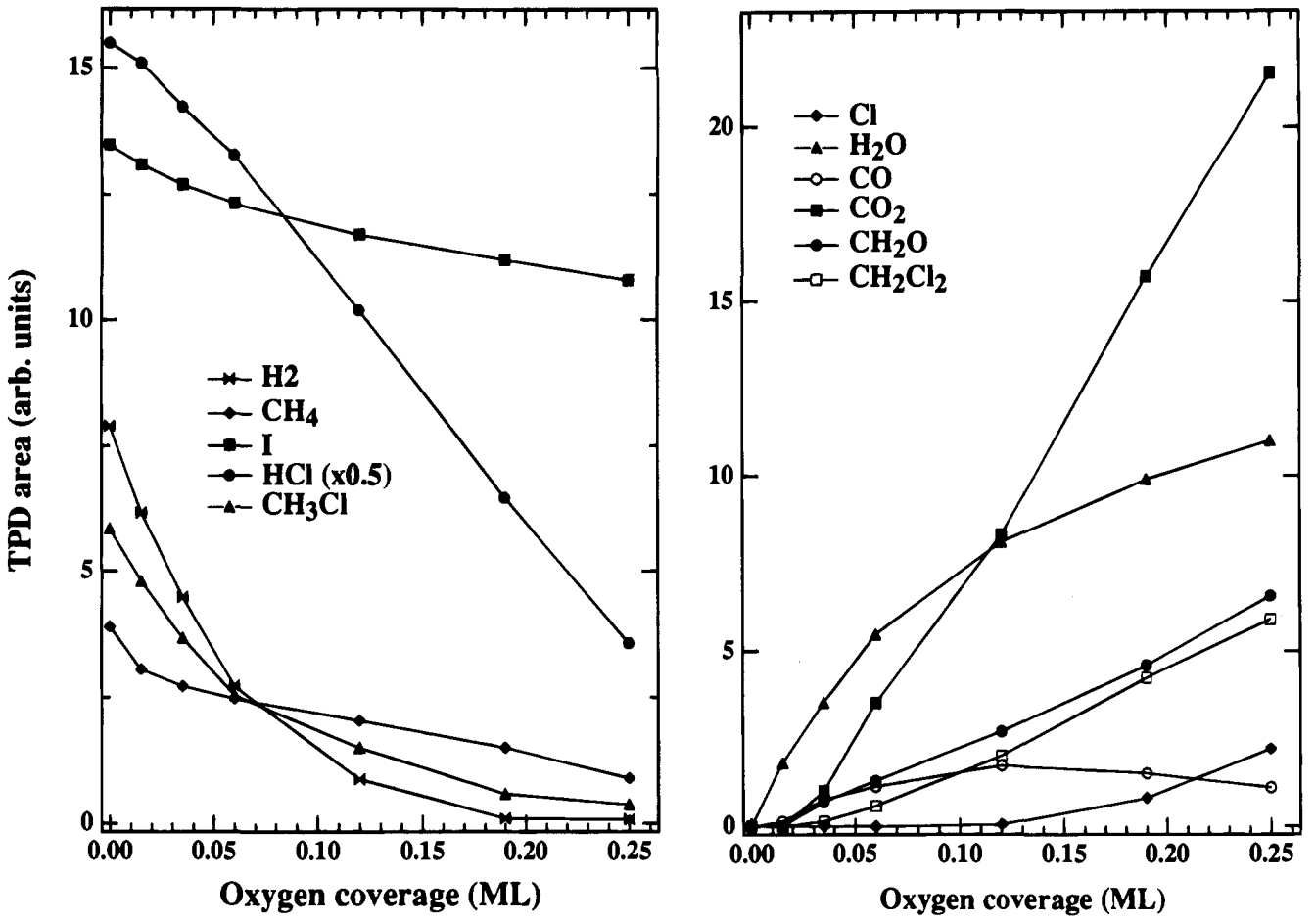

Figure 18. Summary of TPD areas as a function of ^{18}O coverage (from Figure 17).

agreement with literature.[53a] After adsorbing $ClCH_2I$, the 100 K spectrum is identical to that on the clean surface except for the shoulder at 460 cm^{-1} (due to Pt-O stretching). As when O(a) is absent, heating to 170 K shows an additional peak at 1440 cm^{-1} and a shoulder at 2855 cm^{-1}. When the surface is further heated to 210 K, no other significant changes occur except for the emergence of a weak peak at 300 cm^{-1} due to Pt−Cl stretching. As expected, at 250 and 280 K, the Cl(a) intensity is stronger, while the losses associated with $ClCH_2I$ are weaker. There are also changes in the C−H stretching region; a peak at 2940 cm^{-1} emerges. Heating to 320 K eliminates all the loss features due to molecular $ClCH_2I$, consistent with TPD (Figure 16), increases the intensity at 2940 cm^{-1} and decreases the intensity at 460 cm^{-1}. The other losses observed at 320 K are at 300, 460, 770, 1440, and 2855 (shoulder) cm^{-1}. Heating at 370 K eliminates the weak losses at 1440 and 2855 cm^{-1}, reduces the loss intensities at 300, 460, 770, and 2940 cm^{-1}, and introduces two new losses at 850 and 3050 cm^{-1}. At 500 K, only a weak Pt−Cl stretching signal at 300 cm^{-1} is detected; all the other loss features disappear, in harmony with TPD (Figure 16) that shows desorption of only Cl and I above 500 K [I(a) has never been detected with HREELS in this study].

An important point can be made from the HREELS data, i.e., there is no loss peak that can be assigned to ν(C−O) (1000−1400 cm^{-1}), ν(C=O) (1600−2200 cm^{-1}), or ν(O−H) (3200−3600 cm^{-1}). This indicates that possible *oxygen-containing* intermediates which have dipole-active C−O and O−H stretching modes, such as H_2O, OH, CO, and OCHO (formate) [53b−d], do not accumulate on the surface from the reaction of $ClCH_2I$ with O(a). The accumulation of another intermediate, di-σ-bonded $-OCH_2-$, which we propose is a primary reaction intermediate (see section 4.3.), cannot be ruled out based on the HREELS data because its C−O bond is parallel to the surface and, thus, dipole-inactive. However, its accumulation is ruled out by the fact that dosed CH_2O decomposes to CO and H on Pt(111) even at 105.[56] These facts indicate that the desorption kinetics of all the oxidation products are reaction limited.

4. Discussion

4.1. Reactions of $ClCH_2I$ on Clean Pt(111). We turn now to a discussion of the reaction pathways followed by $ClCH_2I$ adsorption on Pt(111). For *monolayer* $ClCH_2I$, Scheme 1 provides a summary. Moving from top to bottom, the temperature increases from 85 to 800 K, as indicated along the left-hand side. For each temperature regime, proposed surface species are listed in the ovals, TPD products in the rectangles, and reaction events on the horizontal lines.

Beginning at the top (85 K), both XPS and HREELS results provide solid evidence that molecular adsorption dominates throughout the monolayer range. In TPD, however, parent

(53) (a) Zhu, X.-Y.; Hatch, S. R.; Campion, A.; White, J. M. *J. Chem. Phys.* **1989**, *91*, 5011. (b) Mitchell, G. E.; Schulz, M. A.; White, J. M. *Surf. Sci.* **1988**, *197*, 379. (c) Columbia, M. R.; Crabtree, A. M.; Thiel, P. A. *J. Am. Chem. Soc.* **1992**, *114*, 1231. (d) Avery, N. R. *Appl. Surf. Sci.* **1982**, *11/12*, 774.

(54) Oxton, I. A.; Powell, B. D.; Sheppard, N.; Burgess, K.; Johnson, B. F. G.; Lewis, J. *J. Chem. Soc., Chem. Common.* **1982**, 719.

(55) Motyl, K.; Norton, J. R.; Schauer, C. K.; Anderson, D. P. *J. Am. Chem. Soc.* **1982**, *104*, 7325.

(56) Henderson, M. A.; Mitchell, G. E.; White, J. M. *Surf. Sci.* **1987**, *188*, 206.

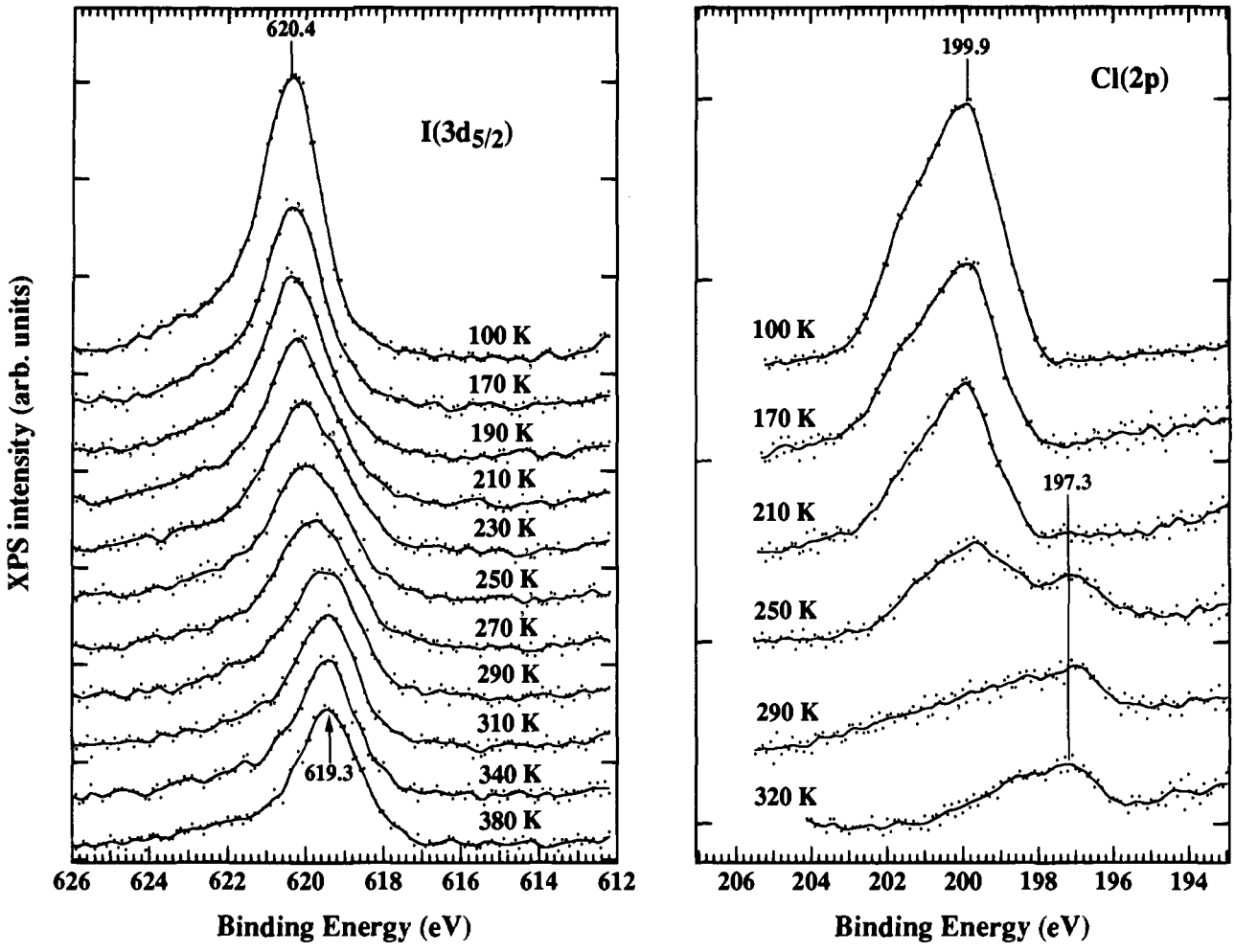

Figure 19. Cl(2p) and I($3d_{5/2}$) XPS for a multilayer $ClCH_2I$ dosed onto 0.25 ML of atomic oxygen and heated to the indicated temperatures.

desorption appears only for coverages above half-monolayer, with peaks at 175 and 233 K. For lower coverages, TPD, with and without coadsorbed D(a), reflects dissociation during heating; adding D(a) enhances the amount of parent desorption and lowers the desorption temperature. Starting at 150 K, there is XPS evidence for I(a), but not Cl(a), i.e., activated C−I cleavage occurs leaving products with the C−Cl bond intact. Methyl chloride desorption at 190 K, especially CH_2DCl(g) which dominates when D(a) is preadsorbed, supports CH_2Cl-(a) as an important dissociation product. C-Cl dissociation is also activated but begins at higher T (170 K) and is signaled by the onset of CH_4 desorption. Accumulation of some Cl(a) is confirmed by XPS and HREELS data taken after heating to 200−230 K. Methane desorption is attributed to hydrogenation of CH_2(a). This conclusion is supported by isotope tracing summarized in Figures 12 and 13; when D(a) is dominant, CH_3D and CH_2D_2 overwhelmingly dominate on the leading edges of the methane TPD, i.e., at ~200 K. POTPD, scavenging of H(a) by tiny amounts of O(a), confirms that H, attributed to C−H cleavage, starts becoming available at 180 K, presumably producing CH(a) and H(a). At 190 K, the reactions H(a) + Cl(a) → HCl(g) and 2H(a) → H_2(g) become activated. All these hydrogenation processes become rapid above 200 K.

Between 150 and 260 K, several kinetically competitive pathways are important. Among them are the following:

(1) C−I bond dissociation competing with parent molecule desorption

(2) hydrogenation of CH_2Cl competing with Cl−C bond dissociation

(3) hydrogenation competing with dehydrogenation of CH_2-(a)

With regard to the second of these, hydrogenation has a lower activation energy (occurs at a lower temperature). Above 210 K, however, the C−Cl dissociation rate dominates. Note, in Figure 2, that the CH_3Cl desorption drops steeply above 210 K even though more $ClCH_2I$ molecules dissociate (see Figure 7) and many C−H bonds break (as evidenced by intense CH_4, CH_3-Cl, and HCl desorption) to provide H. Apparently, above 210 K, once the C−I bond breaks, the activation requirement for C−Cl cleavage is immediately realized so that hydrogenation to form CH_3Cl can no longer compete.

Between 150 and 200 K, a number of important intermediates have been identified. I(a) and Cl(a) were identified by XPS. Cl(a) was also confirmed by the appearance of a 300 cm^{-1} band in HREELS. Other emerging HREELS losses (1440 and 2900 cm^{-1}) at 170 K are taken as evidence for $ClCH_2$(a), consistent both with TPD that shows desorption of CH_3Cl, a hydrogenation product of $ClCH_2$, and with XPS that shows extensive cleavage of C−I, but not C−Cl, bonds. One expects other losses due to $ClCH_2$, e.g., C−Cl and C−Pt stretching but these very likely are buried under the intense features associated with remaining parent $ClCH_2I$.

After heating to 260 K, there is HREELS evidence for the accumulation of CH(a) fragments. Besides CH(a), some CH_2-(a) fragments also survive. Tables 3 and 4 compare the vibrational frequencies assigned to CH_2(a) and CH(a), respectively, on Pt(111) and other surfaces. CH_3(a) is not considered; it is excluded by the absence of an expected intense loss at 1165

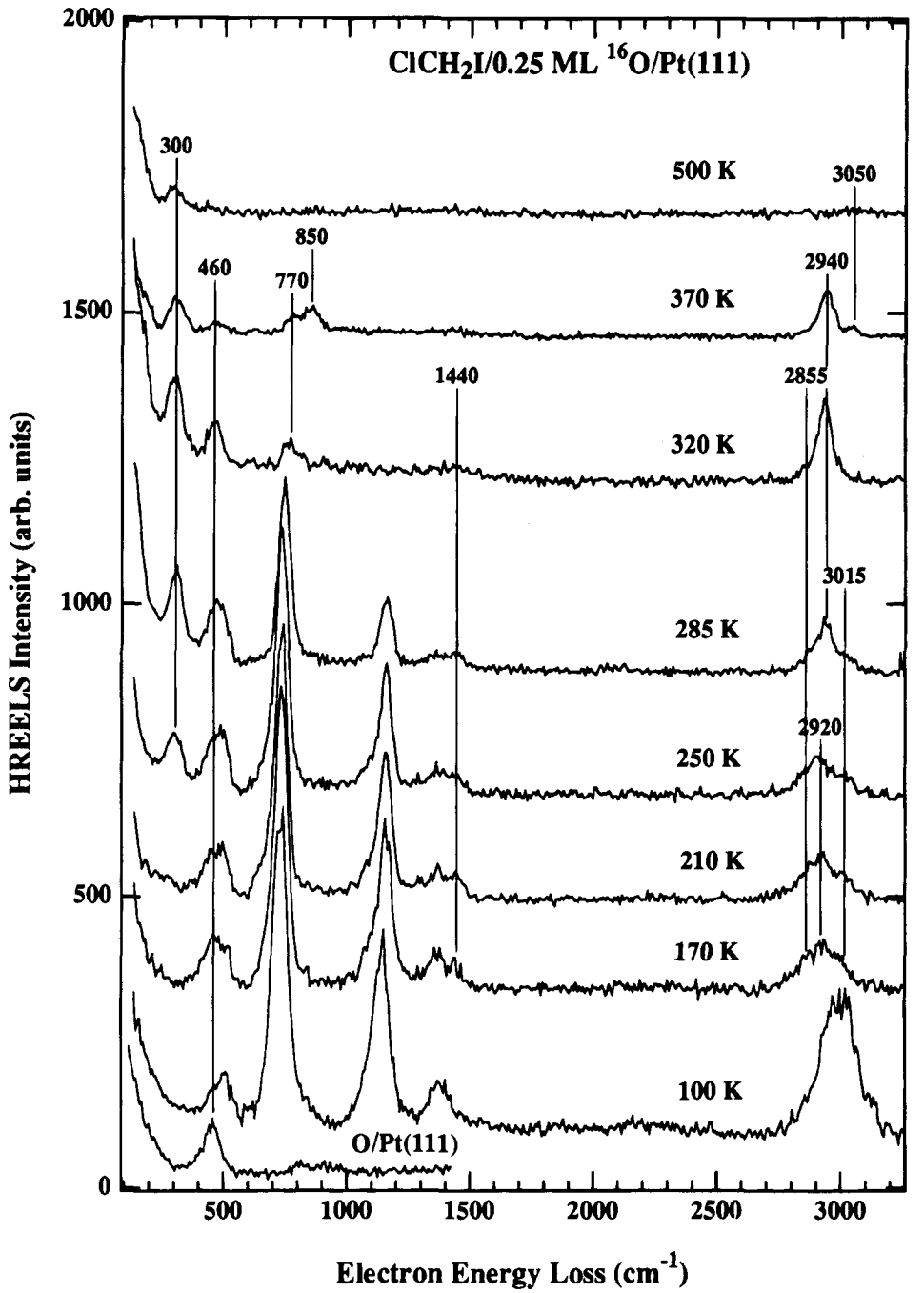

Figure 20. HREELS spectra for a multilayer dose of $ClCH_2I$ onto 0.25 ML of atomic oxygen at 100 K and warmed briefly to various temperatures as indicated.

cm^{-1}.[14,24] While the wagging, twisting, and rocking modes of CH_2(a) have been observed on Ru(001)[33,34] and Fe(110),[35] they are not found in the present case, perhaps due to symmetry (C_{2v}) considerations (see Chart 1). If the noisy peak at 2990 cm^{-1} in Figure 9 is a real feature, then it has to be assigned to the asymmetrical CH_2 stretching, which might result from the impact scattering of the C_{2v} CH_2(a). The HREELS features at 2940, 775, and 480 cm^{-1} are typical of CH(a) whose vibrational characteristics are very well documented (Table 4).

Turning to the structure of CH(a), the intense C−H stretching at 2940 cm^{-1} for CH(a) suggests sp^3 hybridization at the carbon[60] and, sensibly, that CH is bound at threefold Pt sites with the C−H bond perpendicular to the surface (Chart 2). In this orientation, the C−H stretching mode is normal to the surface and, thus, dipole-active, while the C−H bending mode is parallel to the surface normal and dipole-inactive. In this geometry, the relatively weak C−H bending (775 cm^{-1}, Figure 8), compared to the intense C-H stretching, would be attributed to impact scattering. Similar observations and interpretations have been reported for CH on Ru(001)[60] and Ni(111).[64] Alternatively, the C−H bond may be tilted away from the surface normal. Although such an orientation would allow both the C−H bending and stretching to be dipole-active, it is not favored from an energetic point of view. In Chart 2, the three

(57) Baro, A. M.; Ibach, H. *J. Chem. Phys.* **1981**, *74*, 4194.
(58) Hills, M. M.; Parmenter, J. E.; Mullins, C. B.; Weinberg, W. H. *J. Am. Chem. Soc.* **1986**, *108*, 3554.
(59) Parmenter, J. E.; Hills, M. M.; Weinberg, W. H. *J. Am. Chem. Soc.* **1986**, *108*, 3563.
(60) Barteau, M. A.; Broughton, J. Q.; Menzel, D. *Appl. Surf. Sci.* **1984**, *19*, 92. Barteau, M. A.; Feulner, P.; Stengl, R.; Broughton, J. Q.; Menzel, D. *J. Catal.* **1985**, *94*, 51.
(61) Seip, U.; Tsai, M.-C.; Kuppers, J.; Ertl, G. *Surf. Sci.* **1984**, *147*, 65.

Scheme 1

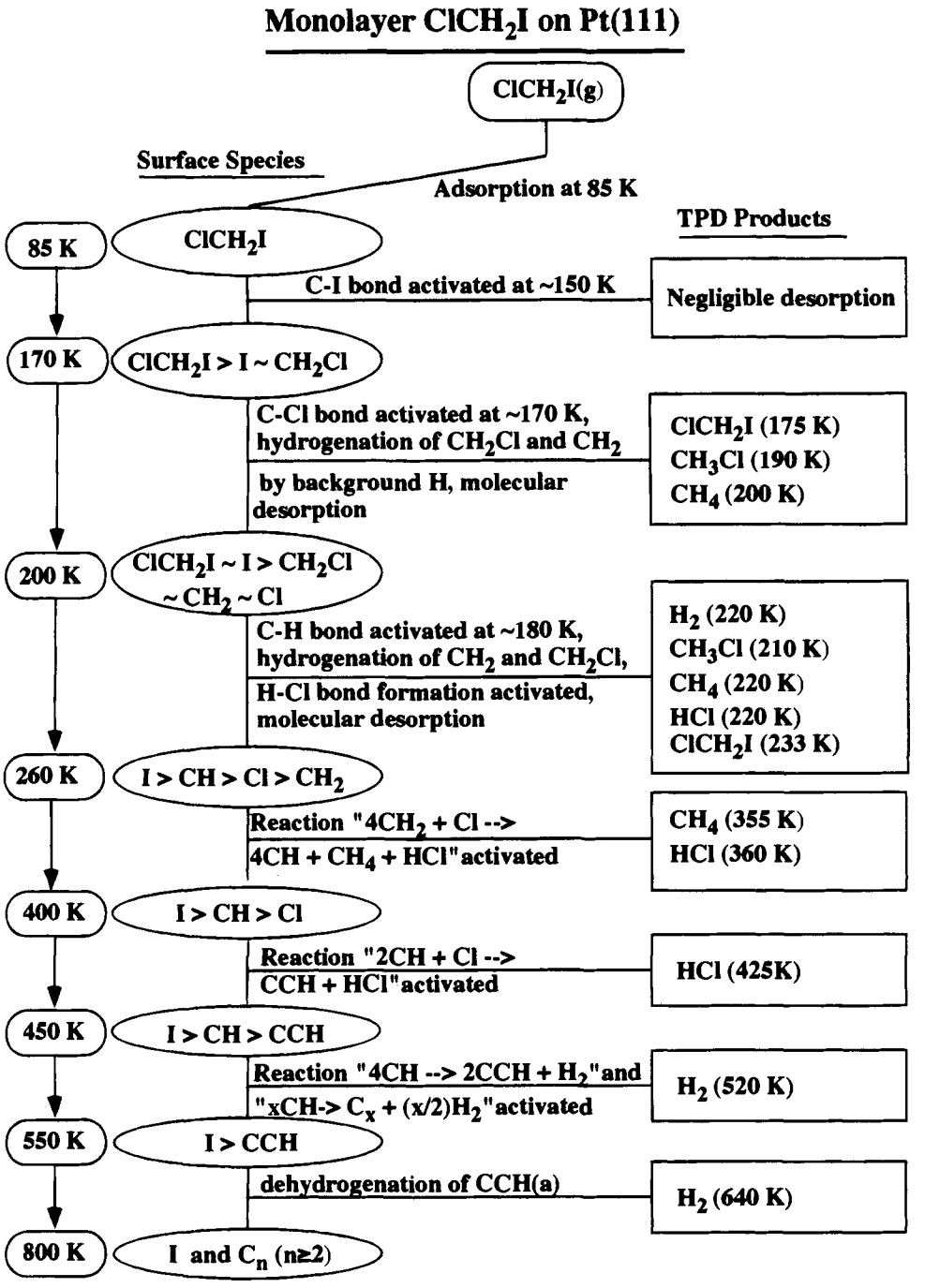

Table 3. Vibrational Frequencies (cm^{-1}) Assigned to CH_2 Species

mode	$CH_2/ClCH_2I/Pt(111)^a$	$CH_2/CH_2CO/Ru(001)^b$	$CH_2/CH_2CO/Fe(110)^c$	$CH_2/CH_2N_2/Ru(001)^d$	$CH_2/CH_2N_2/W(100)^e$	$CH_2/CH_3I/Ru(001)^f$	$CH_2CH_3I/Si(100)^g$	complex(I)[h]	complex(II)[i]
ν_{as}(CH)	2990	2945		3050			2970	2984	2958
ν_s(CH)	2880	2870	2970	2940	2950	2920	2920	2935	2933
$\delta(CH_2)$	1440	1295	1420	1450	1440	1350		1428	
$\omega(CH_2)$		1065	1020	1135		1140		961	943
$\tau(CH_2)$			930	900				869	
$\varrho(CH_2)$		890	790	775		740		811	780
ν_{as}(MC)				650				660	635
ν_s(MC)		590	650	460					467

[a] This work. [b] Reference 34. [c] Reference 36. [d] Reference 33. [e] Reference 35. [f] Reference 38. [g] Reference 7. [h] $(\mu_2\text{-H})_2Os_3(CO)_{10}(\mu_2\text{-CH}_2)$, ref 54. [i] $OS_2(CO)_8CH_2$, ref 55. [j] ν_{as}, asymmetric stretching; ν_s, symmetric stretching; δ, deformation or scission; ω, wagging; τ, twisting; ϱ, rocking.

sp^3 orbitals of the carbon are optimally oriented to interact with the underlying metal orbitals. In passing, we note that on some metal surfaces[57-62,65] (Table 4), where CH has been proposed, the C−H stretching occurs above 3000 cm^{-1} and is weaker than the C−H bending. One explanation is that the carbon atom is sp^2 hybridized and bridges two neighboring metal atoms with

(62) Erley, W.; Baro, A. M.; Ibach, H. *Surf. Sci.* **1982**, *120*, 273.

Table 4. Vibrational Frequencies (cm^{-1}) Assigned to CH Species

mode	CH/$ClCH_2I$/ Pt(111)[a]	CH/CH_2CO/ Pt(111)[b]	CH/H_2CO/ Pt(111)[c]	CH/C_2H_4/ Pt(111)[d]	CH/CH_3I/ Pt(111)[e]	CH/CH_2CO/ Ru(001)[f]	CH/C_2H_4/ Ru(001)[g]	CH/CH_3I/ Ru(001)[h]	CH/C_2H_2/ Ru(001)[i]	CH/C_2H_4/ Ru(100)[j]
ν(CH)	2940	2946	2955	3100	2955	2995	3010	3000	3010	3030
δ(CH)	775		740	850	770	780	810	770	800	790
ν(MC)	480	425			640		465		440	450

mode	CH/H_2+C/ Ru(001)[k]	CH/C_2H_2/ Fe(111)[l]	CH/C_2H_2/ Fe(110)[m]	CH/C_2H_2/ Ni(111)[n]	CH/CH_3/ Ni(111)[o]	CH/C_2H_2/ Rh(111)[p]	CH/CH3I/ Al(111)[q]	CH/CH_3I/ Si(100)[r]	complex(I)[s]	complex(II)[t]
ν(CH)	2950	3015	3050	2980	2970	3025	2930	2970	2988	3041
δ(CH)	720	795	870	790	1275	770	760	945	894	850
ν(MC)			310		650		760		(670,424)	(715,417)

[a] This work. [b] Reference 27. [c] Reference 56. [d] Reference 57. [e] Reference 14. [f] Reference 34. [g] Reference 58. [h] Reference 38. [i] Reference 59. [j] Reference 58. [k] Reference 60. [l] Reference 61. [m] Reference 62. [n] Reference 63. [o] Reference 64, note: there was a loss peak at 750 cm^{-1}; and it was assigned to asymmetric Ni−H stretching rather than to C−H bending. [p] Reference 65. [q] Reference 66. [r] Reference 7. [s] $(CO)_9H_3Ru_3(\mu_3\text{-CH})$ (670 and 424 cm^{-1} are symmetric and asymmetric Ru−C stretching, respectively), ref 67. [t] $(CO)_4Co_3(\mu_3\text{-CH})$ (715 and 417 cm^{-1} are symmetric and asymmetric Co−C stretchings, respectively), ref 68.

Chart 2

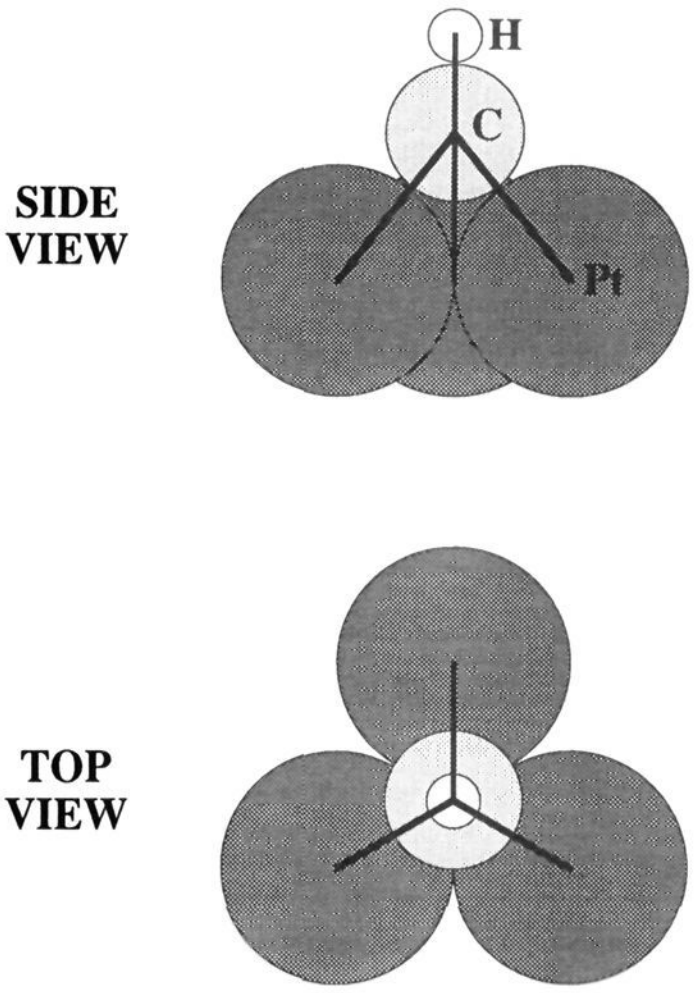

Chart 3

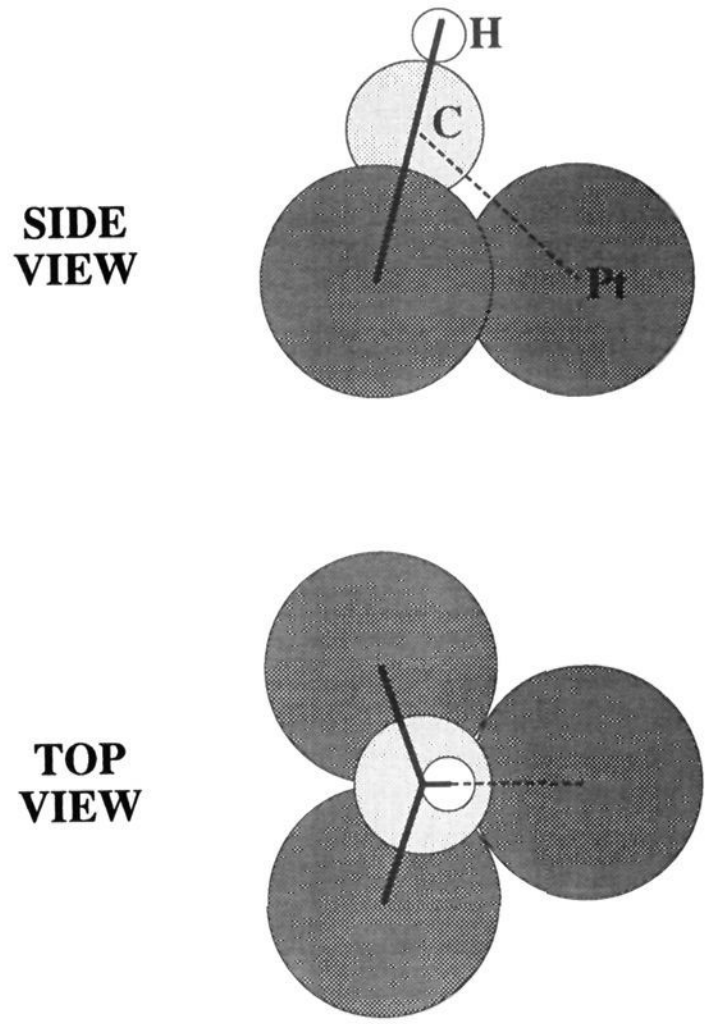

the C−H bond inclined away from the surface normal (see Chart 3).[63] An alternative, involving η^2-CCH(a), should also be considered (see discussion below).

The CH_2(a) that remains at 260 K disappears by 370 K (HREELS evidence). Desorption of CH_4 and HCl in the range 355−360 K points to further dehydrogenation (i.e., $CH_2(a) \rightarrow CH(a) + H(a)$) and hydrogenation (i.e., $CH_2(a) + 2H(a) \rightarrow CH_4(g)$ and $H(a) + Cl(a) \rightarrow HCl(g)$) competing and both removing CH_2(a). Based on relative TPD areas in the 355 K temperature range, we estimate that 0.021 ML of CH_2(a) is present at 260 K. It is not clear why this amount survives, while the majority (0.088 ML, refer to Table 2) reacts at lower temperature. While coadsorbed halogens may play some role, we note that for CH_2N_2, i.e., no halogens, on Pt(111), CH_4 desorption also extended to high temperature (400 K). Thus, other factors, e.g., local adsorbate structural organization, may be important.

Continuing with scheme 1, at 400 K, the species remaining on the surface are I(a), Cl(a), and CH(a). The Cl(a) desorbs as HCl at 415 K (Figure 4), the hydrogen atoms coming from CH(a). The attenuation of CH(a) vibrational modes supports this proposal. Stoichiometric balance also points to CH(a); the H_2 desorbed above 400 K, for ≥200 s exposures, corresponds to 0.088 ML H(a). The coverage of C(a) retained at 1000 K is 0.102 ML. The difference between C(a) and H(a), 0.014 ML, nearly equals the 0.019 ML of HCl that desorbs at 415 K. The emergence, at 450 K, of new loss features (830 and 3035 cm^{-1}), indicates that HCl formation is accompanied by a reaction other than conversion of CH(a) to C(a). We propose a reaction producing HCl(g) + CCH(a). More CCH(a) appears at 540 K, but at 640 K it dehydrogenates, leaving carbon on the surface and yielding a broad H_2 peak centered at 640 K.

Turning to the surface species responsible for the vibrational peaks at 830 and 3035 cm^{-1}, there is good evidence for η^2-

(63) Demuth, J. E.; Ibach, H. *Surf. Sci.* **1978**, *78*, L238. Lehwald, S.; Ibach, H. *Surf. Sci.* **1979**, *89*, 425. Erley, W.; McBreen, P. H.; Ibach, H. *J. Catal.* **1983**, *84*, 229.

(64) Ceyer, S. T. *Langmuir* **1990**, *6*, 82.

(65) Dubios, L. H.; Somorjai, G. A. In *Am. Chem. Soc. Symp. Ser.*, Bell, A. T., Hair, M. L., Eds.; American Chemical Society: Washington, DC, 1980.

(66) Chen, J. G.; Beebe, T. P., Jr.; Crowell, J. E.; Yates, J. T., Jr. *J. Am. Chem. Soc.* **1987**, *109*, 1726.

(67) Oxton, I. A. *Spectrochim. Acta, Part A* **1982**, *38*, 181.

(68) Howard, M. W.; Kettle, S. F.; Oxton, I. A.; Powell, D. B.; Sheppard, N.; Skinner, P. *J. Chem. Soc., Faraday Trans. 2* **1981**, *77*, 397.

Chart 4

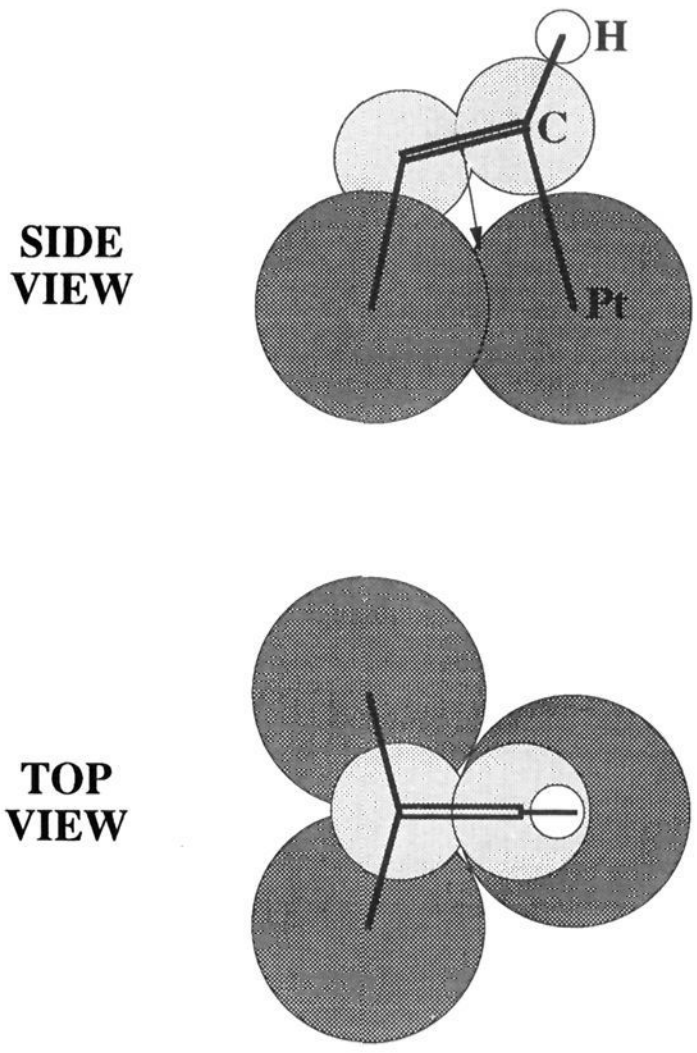

CCH(a) (see Chart 4). In the chemistry of C_2H_3I on Pt(111), ethylidyne [CCH_3(a)] forms below and partially dehydrogenates above 450 K, producing two H_2 desorption peaks (520 and 650 K).[6] As here, the partially dehydrogenated species gives losses at 835 and 3035 cm^{-1}. Ethylene on Pt(111), heated to 620 K, dehydrogenates to leave a stoichiometry of C:H = 2:1 and two losses at 850 and 3100 cm^{-1}.[57] The nature of the intermediate(s) has been, however, somewhat controversial. Baro and Ibach[57] proposed C(a) and CH(a). Salmeron et al.[69] and Davis et al.,[70] proposed mixtures of CCH(a), CH(a), and C(a) from their TPD and ^{14}C radiotracer study. Zhou et al.,[71] using SSIMS, provided evidence for C−C bonds throughout the entire dehydrogenation process. Recent work by Land et al.,[72] using STM, showed C−C bonds (clusters) upon completion of ethylidyne dehydrogenation (700 K) and graphite island formation at higher temperatures. Thus, while some CH(a) may be present, the evidence favors CCH(a) as the dominant species between 540 and 640 K. The fact that both the decomposition of CCH_3(a) and the reaction of $ClCH_2I$ on Pt(111) give the same HREELS spectra above 500 K indicates that, in the latter case, CCH(a) is also a likely intermediate.

A simple comparison of the electron energy losses at 830 and 3035 cm^{-1} (Figure 8) with literature[57−62,65] (see Table 4) may lead, erroneously, to a conclusion that the new surface species above 450 K is also CH(a). To support this conclusion, one would have to argue that a rehybridization from sp^3 to sp^2 of the carbon in CH(a) had occurred. However, such a rehybridization is not thermodynamically favored.[73]

On the other hand, introducing η^2-CCH(a) makes for a consistent picture. Forming CCH(a) is thermodynamically favored ($\Delta H = -20$ kcal/mol).[74] The carbon atoms in η^2-CCH(a) would be sp^2 hybridized, and, as anticipated, the stretching frequency (3035 cm^{-1}) is higher than sp^3 (2940 cm^{-1}). The stretching frequency is, in fact, the same as for sp^2 carbons in acetylene on Pt(111).[50,75] For comparison, we show in Table 5 the observed vibrational frequencies assigned to CCH species in $Os_3(CO)_9(\mu\text{-H})(\mu_3\text{-}\eta^2\text{-CCH})$ and on several metal surfaces.

The absence of a C−C stretch for η^2-CCH(a) in Figure 8 is not entirely unexpected; this mode often gives a very weak and broad peak.[77,80] If, as might be expected, the C−C bond lies nearly parallel to the surface, dipole scattering will be weak. Moreover, the estimated coverage of CCH(a) does not exceed 0.04 ML (based on the 640 K H_2 TPD area), probably below our detection limit.[82] Difficulty distinguishing *CH* and *CCH* fragments has arisen in other work.[6,57,76,77] Based on a broad peak between 1100 and 1500 cm^{-1} [6,57] which can be assigned to the C−C stretching in η^2-CCH(a), we reinterpret our earlier HREELS results for C_2H_3I on Pt(111)[6] in these terms (see Table 5). Similarly, some earlier assignments to CH(a) (Table 4) may need to be reconsidered.

Species other than CCH(a) and CH(a) must be involved at 520 K. Before the 520 K H_2 peak starts to desorb, 0.017 ± 0.003 ML CCH(a) and 0.069 ± 0.005 ML CH(a) are present. Assuming CCH(a) formation accompanies the 520 K H_2 peak, its peak area requires decomposition of ~0.051 ML of CH(a). The last hydrogen desorbs at 640 K, and the above proposal would lead to an H_2 peak area ratio (520 K area/640 K area) of 0.3−0.35, much smaller than observed (~1.0, Figure 5). To account for this, we propose that reactions leading to clusters of carbon, C_x(a), are also occurring.

Because both invoke CH_2(a), a comparison of our results with those for CH_2N_2 on Pt(111)[28] is in order. There are similarities and differences. First, while only CH_2 accumulates when CH_2N_2 is used, CH_2, Cl-bearing species, and I accumulate for $ClCH_2I$. Thus, when using diazomethane, we expect that a higher local coverage of neighboring CH_2 will be easily realized; linking these groups could account for the observed ethylene desorption. On the other hand, when using $ClCH_2I$, access of CH_2 groups to each other may be inhibited by the presence of halogens, thereby accounting for the absence of ethylene desorption. In this regard, the following points should be considered. First, Pt is an effective catalyst for C−H and C−C bond breaking and, except at high coverage where most Pt sites are occupied, is not effective for C−C bond formation. Thus, it is likely that total coverage of C-containing species is important in the diazomethane case. The importance of coverage is illustrated by CH_3(a) on Pt(111); carbon−carbon coupling to form CCH_3(a) occurred only when the initial CH_3 coverage was high.[21] In this context, it is noteworthy that the

(69) Salmeron, M.; Somorjai, G. A. *J. Phys. Chem.* **1982**, *86*, 341.
(70) Davis, S. M.; Zaera, F.; Gordon, B. E.; Somorjai, G. A. *J. Catal.* **1985**, *92*, 240.
(71) Zhou, X.-L.; Zhu, X.-Y.; White, J. M. *Surf. Sci.* **1988**, *193*, 387.
(72) Land, T. A.; Michely, T.; Behm, R. J.; Hemminger, J. C.; Comsa, G. *Appl. Phys.* **1991**, *A53*, 414.

(73) For sp^3 CH on Pt(111), there are three σ Pt−C bonds worth 159 kcal/mol, and for sp^2 CH there are two σ Pt−C bonds worth 106 kcal/mol.[74] If the C−H bond is perpendicular to the surface, the *p* orbital of the sp^2 carbon is parallel to the surface, and its interaction with Pt 6*s* and 5*d* orbitals will be negligible. The orbital interaction can be increased by tilting the C−H bond from its perpendicular position (Chart 3) but will not reach that between the sp^3 orbital of carbon and Pt 6*s* and 5*d* orbitals. By analogy, π(C−C) bonds are always weaker than σ(C−C) bonds.
(74) Carter, E. A.; Koel, B. E. *Surf. Sci.* **1990**, *226*, 339.
(75) Ibach, H.; Lehwald, S. *J. Vac. Sci. Technol.* **1978**, *15*, 407.
(76) Gates, J. A.; Kesmodel, L. L. *Surf. Sci.* **1982**, *120*, L461; **1983**, *124*, 68.
(77) Kesmodel, L. L.; Waddill, G. D.; Gates, J. A. *Surf. Sci.* **1984**, *138*, 464.
(78) Stroscio, J. A.; Bare, S. R.; Ho, W. *Surf. Sci.* **1983**, *148*, 499.
(79) Bent, B. E.; Mate, C. M.; Crowell, J. E.; Koel, B. E.; Somorjai, G. A. *J. Phys. Chem.* **1987**, *91*, 1493.
(80) Slavin, A. J.; Bent, B. E.; Kao, C.-T.; Somorjai, G. A. *Surf. Sci.* **1988**, *206*, 124.
(81) Evans, J.; McNulty, G. S. *J. Chem. Soc., Dalton Trans.* **1984**, 79.
(82) Griffiths, K.; Lennard, W. N.; Mitchell, I. V.; Norton, P. R.; Pirug, G.; Bonzel, H. P. *Surf. Sci.* **1993**, *284*, L389.

Table 5. Vibrational Frequencies (cm^{-1}) Assigned to CCH Species[l]

mode	$C_2H/ClCH_2I/Pt(111)$[a]	$C_2H/C_2H_3I/Pt(111)$[b]	$C_2H/C_2H_4/Ru(001)$[c]	$C_2H/C_2H_2/Pd(111)$[d]	$C_2H/C_2H_2/Pd(100)$[e]	$C_2H/C_2H_4/Ni(110)$[f]	$C_2H/C_3H_6/Rh(111)$[g]	$C_2H/C_2H_4/Rh(100)$[h]	$Os_3(CO)_9(\mu\text{-H})(\mu_3\text{-}\eta^2\text{-CCH})$[i]
ν(CH)	3035	3035	2960	2995	3030	2990	3020	3025	3157
ν(CC)		1300[k]	1290	1360	1360	1290	1380	1305	1534
δ(CH)	830	835	750	750	750	890	815	805	(861,854)[j]
ν_{as}(MC)						465	490	430	
ν_s(MC)			435			380		370	

[a] This work. [b] Reference 6. [c] Reference 58. [d] Reference 76 and 77. [e] Reference 77. [f] Reference 78. [g] Reference 79. [h] Reference 80. [i] Reference 81. [j] Doublets. [k] A broad peak between 1100 and 1500 cm^{-1}. [l] ν_{as}, asymmetric stretchings; ν_s, symmetric stretching; δ, bending.

saturation CH_2(a) coverage produced from CH_2N_2[28] is at least four times higher than produced by dissociation of $ClCH_2I$. However, C_2H_4 was still observed in TPD when only 0.048 ML CH_2N_2 was adsorbed on Pt(111).[28] *Local* coverage remains an attractive possibility; for $ClCH_2I$ decomposition, the CH_2 fragments may seldom escape from halogens which, through steric effects, could inhibit recombinative formation of C_2H_4. While the role of halogens may be important here, it is not universal. On Ag(111),[19] Cu(110),[29] and Pd(100),[4] coupling of CH_2(a) to form C_2H_4(g) occurs readily in the presence of coadsorbed halogens.

Dihydrogen formation and desorption is not altered significantly by the presence of halogens; both diazomethane and chloroiodomethane lead to two identical H_2 peaks above 500 K and to distinguishable H_2 desorption only at lower temperatures (200–290 K).[28] In our case, the low temperature H_2 peak (220 K) is reaction-limited (i.e., kinetically controlled by the dehydrogenation of CH_2(a) and/or CH_2Cl(a)). It is weak because much of the H(a) is removed at lower temperatures as either HCl or CH_3Cl. For CH_2N_2, the low temperature H_2 peak (290 K) was attributed primarily to dehydrogenation and subsequent rearrangement of C_2H_4 to CCH_3.[28] We find that CH_2 starts to dehydrogenate at 180 K but becomes rapid only above 200 K. Assuming the same for CH_2 derived from CH_2N_2, then part of the 290 K H_2 desorption is attributable to C–H cleavage at lower temperature, i.e., it is not solely due to dehydrogenation of C_2H_4 to form CCH_3. This is supported by the fact that, when H_2 was coadsorbed with CH_2N_2 on Pt(111), the dosed hydrogen also desorbed at 290 K.

At higher temperatures, we have presented evidence that the 640 K peak is attributable to CCH(a) decomposition; the same species likely controls the high temperature region when diazomethane is used. The 520 K peak is attributed to different dominant sources in the two cases—CCH_3(a) in the case of CH_2N_2 and CH(a) for chloroiodomethane. As mentioned earlier, the dehydrogenation of CCH_3 on Pt(111) produces two H_2 peaks[6] just as CH(a) does. Obviously, similar TPD spectra, by themselves, do not establish that the same intermediates are in control. However, our TPD and HREELS data indicate that complete decomposition of CH_2(a) to C(a) does not occur below room temperature and, since there is no evidence for CCH_3 accumulation, we have proposed CH(a). While halogens may inhibit ethylene and ethylidyne formation in our case, we see no reason to suppose that CH(a) formation should not participate in the decomposition of CH_2 derived from CH_2N_2. Clearly, direct measurement of intermediates formed from CH_2N_2, e.g., using HREELS, would be very worthwhile.

Like dihydrogen, methane desorption is similar for both adsorbates; strong peaks with shoulders are evident in the 200–270 K regime (Although not discussed,[28] a close look at the TPD spectrum after CH_2N_2 exposure, suggests a shoulder at about 200 K; it is clearer when H is coadsorbed.) This result indicates that the presence of halogens does not dramatically alter the pathway leading to methane. We take this as consistent with the notion that neither C–H bond breaking nor diffusion to hydrogenate CH_2 are inhibited by halogens.

It is interesting that another adsorbate, CH_3I, gives H_2 TPD very much like those for CH_2N_2 and $ClCH_2I$—three H_2 desorption peaks (320, 520, and 640 K).[14,23,24] There is general agreement that the 320 K H_2 peak is limited by recombination of H(a) formed from the dehydrogenation of CH_3(a) at lower temperatures. Earlier work attributed the two higher temperature peaks to dehydrogenation of CH_2(a)[23] or CH(a),[14] but we have proposed dehydrogenation of CH(a) and CCH(a) fragments, respectively, because our data indicate that CH_2(a) is not stable over 300 K. There is positive infrared identification of CH_2 only up to 280 K.[23] Since dehydrogenation and subsequent hydrogenation of CH_3(a) to form methane occur in this same temperature regime, methylene formation from CH_3 is sensible and consistent with our proposal (see scheme 1). We believe that, whether CH_3 or CH_2 is the initial species on Pt(111) at low temperatures, the final thermal reaction intermediates are the same—CH(a) and CCH(a).

Continuing to compare iodomethane and chloroiodomethane, there are some differences in H_2 desorption at low temperatures. At saturation, $ClCH_2I$ gives a very small H_2 peak at 220 K, while CH_3I gives a large H_2 peak at 320 K. Local coverage appears to be important—as C–I and C–Cl bonds break in the presence of a locally crowded surface, atomic hydrogen is displaced and recombined immediately to desorb dihydrogen. For $ClCH_2I$, the available H(a) is consumed to form HCl, also at 220 K, making the H_2 desorption in this region negligible.

4.2. Reactions of $ClCH_2I$ with D(a). Within the above framework, the impact of coadsorbed D is readily understood. At low temperatures, D enhances the competitiveness of parent desorption with respect to dissociation. In fact, according to Figure 11, coadsorbed D lowers the thermal activation needed for parent desorption. Since dissociation starts at about 150 K, with or without D(a), the fraction of parent desorbing increases. Even when dissociation occurs, coadsorbed D(a) diminishes the extent to which C-containing fragments end up as fully dehydrogenated surface carbon. Competitive and reversible dehydrogenation and hydrogenation of CH_2(a) and CH_2Cl(a) accounts for this, i.e., increasing the chemical potential of atomic hydrogen increases hydrogenation.

It is interesting that, besides the dominant deuteration products (CH_2D_2 and CH_2DCl), there are also H-D exchange products for methane (CHD_3 and CD_4) but not for methyl chloride. Model structures accounting for this distinction are presented in scheme 2 (The scheme does not imply that adsorbed D promotes C–H and C–Cl bond dissociation.). For CH_2Cl(a), we suppose that the carbon–surface bond is tilted, allowing the Cl atom to interact with the surface, and keep the H atoms away from it.[14] From this geometry, the transition state involving D leads to either CH_2DCl, which desorbs, or CH_2D-(a) and Cl(a). Once broken, the C–Cl bond does not reform. Through the entire reaction process that forms methyl chloride, the two original C–H bonds remain, i.e., neither CHD_2Cl nor

Scheme 2

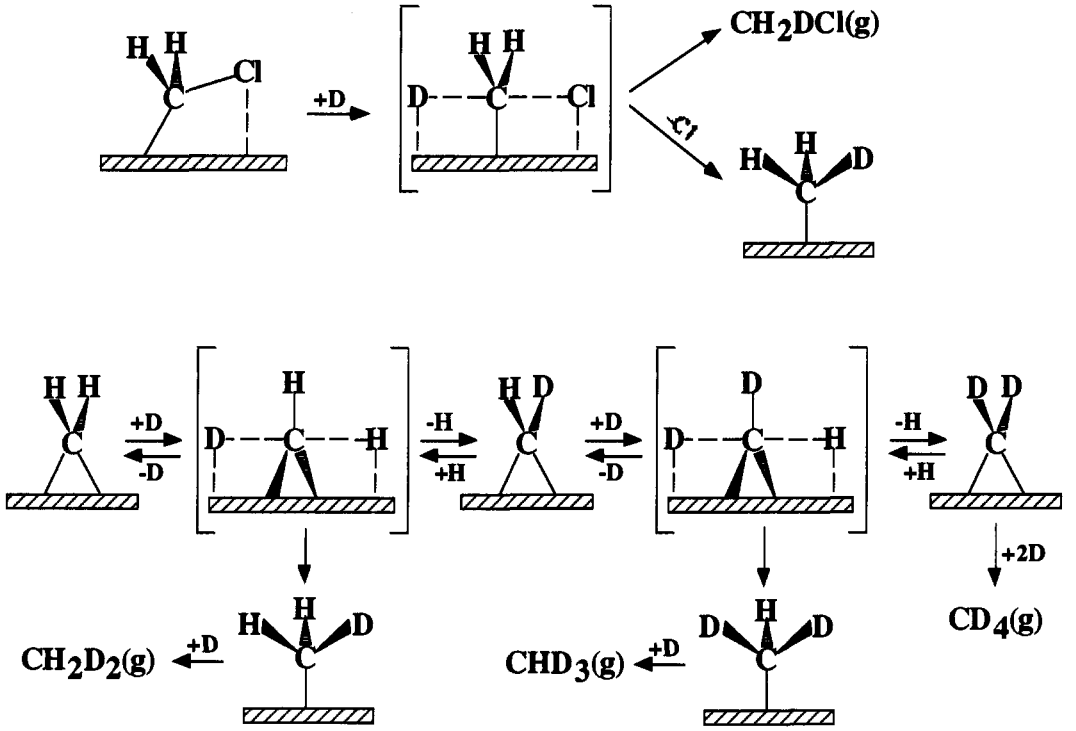

CD_3Cl form. On the other hand, when CH_2 incorporates D(a), the transition state leads to either $CH_2D(a)$ (hydrogenation) or CHD(a) (exchange). Repeated arrival at this transition state would lead to both CHD_3 and CD_4, the distribution being determined by the surface concentration of D(a) and the hydrogenation activity of surface bound methyl groups. There is independent evidence for D-for-H exchange in CH_3 groups; in the presence of a large concentration of D(a), CH_3I reacts on Pt(111) to form CD_4 and CD_3H.[25] These authors proposed a rapid equilibration involving CH(a) and $CH_2(a)$ to account for their observation that more CD_4 than CD_3H desorbed. A similar process may contribute in our case as well, since POTPD indicates that CH_2 break up, beginning at 180 K, becomes rapid above 200 K. In this context, surface defects may play some role in the dehydrogenation of CH_2 below 200 K, but it is not necessary to do so.

Not surprisingly, the D concentration is highest in the lowest temperature peak (194−198 K, Figures 12 and 13). Toward higher temperatures, D(a) is consumed, H(a) is supplied, and the concentration of D in the methane drops. The 355 K methane peak is interesting. Up to a limit, the total desorption in this region intensifies as the initial D(a) coverage increases (compare Figures 3 and 12), but this peak disappears when D(a) is high (Figure 13). For an initial coverage of 0.15 ML D(a), we estimate, from the methane (CH_4, CH_3D and CD_2H_2) peak at 355 K and the HCl peak at 360 K, that a total of 0.01 ML ($CH_2(a)$, CHD(a), and $CD_2(a)$) remains above 300 K, compared to 0.02 ML on the D-free surface. Nevertheless, because less Cl(a) is present at 355 K to abstract H from $CH_2(a)$ to form HCl, more methane is produced, even though the total methylene coverage is lower. Overall, the methane formation here is very similar to that observed when CH_2N_2 was coadsorbed with H(a).[28]

The isotopic content of the 355 K methane peak is also interesting. Figure 12 shows that, even though the H(a) and D(a) present at low temperatures recombine and desorb near 230 K, there is significant D(a) content in the 355 K methane peak. We take this as indicating the formation of a significant concentration of CDH_x (x = 1,2) below 240 K, presumably through an exchange like that illustrated in Scheme 2.

4.3. Reactions of $ClCH_2I$ with Atomic O. As atomic oxygen is added, perturbation of the parent $ClCH_2I$ desorption becomes apparent but only for O(a) ≥ 0.035 ML; the multilayer peak, as expected, remains fixed at ca. 160 K, but the monolayer peak broadens toward higher temperature and splits into at least two identifiable local maxima (240 and 305 K). Because XPS confirms the presence of both C−I and C−Cl bonds, even at 290 K, and because HREELS indicates some molecular $ClCH_2I$ at 285 K, the $ClCH_2I$ TPD peak at 305 K is attributed to molecular $ClCH_2I$ species rather than the recombination of dissociated $ClCH_2I$. Stabilization by O(a) can be readily understood as a donor−acceptor interaction.[83] Like other alkyl halides,[84] $ClCH_2I$ lowers the surface weak function, i.e., is an electron donor. Atomic oxygen, on the other hand, is an electron acceptor and increases the surface work function of Pt(111).[85] Compared to clean Pt(111), some sites become electron deficient in the presence of O(a), and, as a result, the interaction with $ClCH_2I$ increases. The destabilization effect of coadsorbed D can be understood in the same way; atomic D is an electron donor (increases the surface work function of Pt(111)[86]) making some adsorption sites electron rich and weakening the adsorbate−substrate interaction.

More interesting is the participation of O(a) in the reaction chemistry of $ClCH_2I$, particularly the formation of oxidation products. For very low initial O(a) coverages, water (220 K) and carbon monoxide (450 K) desorb, but carbon dioxide and formaldehyde are absent. These two products, and CH_2Cl_2, begin to appear for O(a) ≥ 0.035 ML (recall that saturation O(a) is 0.25 ML). XPS indicates that, just as in the absence of O(a), dissociation starts with C−I bond cleavage below 170 K. The low onset temperature (~155 K) for CH_2O desorption indicates that a few C−Cl bonds are activated below 170 K.

(83) Akhter, S. A.; Zhou, Y.; White, J. M. *J. Chem. Soc., Faraday Trans.* **1990**, *86*, 2271.
(84) Jo, S. K.; White, J. M. *J. Phys. Chem.* **1990**, *94*, 6852.
(85) Ranke, W. *Surf. Sci.* **1989**, *209*, 57.
(86) Christmann, K.; Ertl, G.; Pignet, T. *Surf. Sci.* **1976**, *54*, 365.

However, C−Cl cleavage is not evident in XPS and HREELS, so we conclude that C−Cl bond breaking, accompanied by partial oxidation to formaldehyde, occurs to a much less extent than C−I bond breaking. We suggest that desorption, rather than oxidation, of CH_2O is the result of a stoiciometric shortage of O(a) and a locally high coverage of halogens (Cl and I) which weakens the bonding of CH_2O(a) to the surface. Above 0.35 ML O(a), this trend continues, but complete oxidation to CO_2 becomes more important. Further, no C−H bonds are retained beyond 500 K for oxygen coverages higher than 0.19 ML. HREELS indicates accumulation of $ClCH_2$, and, in TPD, CH_2Cl_2 increases sharply.

While increasing O(a) reduces the intensity of the CH_3Cl, CH_4, and HCl TPD peaks, the peak temperatures are constant (Figure 17). These features can be described in terms of reactions and sites that are not perturbed by O(a). Obviously, other sites and reactions are dependent on O(a), e.g., O(a) competes for available H(a) and stabilizes some $ClCH_2I$ and $ClCH_2$, preserving C−Cl bonds to temperatures where reactions leading to chlorination to Cl_2CH_2 and partial oxidation to CH_2O can compete with HCl, CH_4, and CH_3Cl formation. Starting with saturation O(a) (0.25 ML), the broad I($3d_{5/2}$) XPS peak, observed at 250 K, corresponds to 45% I(a) and 55% molecular $ClCH_2I$(a), compared to 100% I(a) when O(a) is absent. Since no O-containing reaction intermediates associated with the oxidation products were identified with HREELS, we conclude that evolution of these products is reaction-limited and involves CH_2(a) or CH_2Cl(a) since both are present in spectroscopically significant concentrations between 210 and 285 K. Methoxy, CH_3O(a), can be ruled out because no methanol is found in TPD.[52] From all the XPS and HREELS evidence, it appears that dissociation of C−I and C−Cl and the formation of CH_2O proceed simultaneously, resulting in only small changes in the CH_2(a) and CH_2Cl(a) concentrations between 210 and 285 K.

The TPD for CH_2O, H_2O, HCl, CO_2, CH_2Cl_2, and $ClCH_2I$ all peak at the same temperature, 305 K, and, for CH_2O, HCl, CH_2Cl_2, and $ClCH_2I$, cut off sharply at 320 K. In traversing the temperature range between 170 and 320 K, XPS and HREELS data indicate the following: (1) $ClCH_2I$ dissociates, (2) the CH(a) (770 and 2940 cm^{-1}) concentration increases, (3) the Cl(a) concentration remains nearly the same, and (4) at 320 K, the surface coverage includes a small quantity of CH_2(a) but no $ClCH_2I$(a). Based on this information, we propose the following, not necessarily elementary, reactions to form these products:

$$H(a) + Cl(a) \rightarrow HCl(g) \quad (1)$$

$$CH_2Cl(a) + Cl(a) \rightarrow CH_2Cl_2(g) \quad (2)$$

$$2H(a) + O(a) \rightarrow H_2O(g) \quad (3)$$

$$CH_2(a) + O(a) \rightarrow CH_2O(a) \quad (4)$$

$$CH_2O(a) \rightarrow CH_2O(g) \quad (5)$$

$$CH_2O(a) \rightarrow CO(a) + 2\,H(a) \quad (6)$$

$$CH_2O(a) + O(a) \rightarrow -OCHO-(a) + H(a) \quad (7)$$

$$-OCHO-(a) \rightarrow CO_2(g) + H(a) \quad (8)$$

$$CO(a) + O(a) \rightarrow CO_2(g) \quad (9)$$

Alongside these reactions, there is decomposition eventually leading to CCH(a) (Figure 20) and C_x(a), as in Scheme 1. We propose that CH_2O(a), in di-σ-bonded form, $-CH_2O-$, is the key intermediate that leads to formaldehyde, carbon monoxide, and carbon dioxide. The distribution of these products is determined by the local oxygen and halogen coverages; when oxygen is in short supply, partial oxidation of CH_2(a) followed by desorption (reactions 4 and 5) dominate. When the local concentration of oxygen is high, formate (OCHO, reaction 7) forms and promptly decomposes, leading to the sharp 305 K peak for CO_2. While the cut-off (320 K) is the same for CH_2O, H_2O, and CO_2, CH_2O sets in at lower temperatures than either water or carbon dioxide. This can be understood in terms of two kinetically competitive reaction channels for the $-O-CH_2-$. Below 280 K, rearrangement and desorption as CH_2O dominates, i.e., lower activation energy. Above 280 K, reaction to form CO(a) or OCHO(a) begins to dominate. CO_2 is released either from the dehydrogenation of OCHO(a) or the oxidation of CO. Water is produced from the released H(a). This proposal is consistent with the literature. Formate decomposes between 210 and 280 K, producing CO_2(g) and H(a).[87] Methoxy (CH_3O), in the presence of O(a), undergoes dehydrogenation to CO and H beginning at 170 K, and CO_2 evolves at 320 K.[88] CO oxidation sets in around 260 K.[89] Interestingly, whereas CH_2O normally adsorbs dissociatively to form CO and H at 105 K,[56] in our case, coadsorbed halogens modify the surface, so that the decomposition channel of $-OCH_2-$ does not become competitive with desorption until about 280 K. Because both the decomposition of $-OCHO-$ and the oxidation of CO occur at lower temperatures than the proposed reactions that form $-O-CH_2-$(a), spectroscopically significant concentrations of CO(a) and $-OCHO-$(a) do not accumulate, e.g., in Figure 20, there is no evidence for any CO(a).

The peak for parent $ClCH_2I$ at 305 K and, particularly, the sharp cut-off at 320 K suggest that dissociation of $ClCH_2I$ induces the desorption of neighboring species in a process similar to that proposed for the thermal and photodesorption of O_2 from Ag(110).[90]

As shown in Figure 20, heating the surface from 320 to 370 K eliminates all CH_2(a), decreases the amounts of CH(a), Cl(a), and O(a), and causes the formation of CCH(a) (850 and 3050 cm^{-1}). The species desorbing in this temperature regime are HCl, H_2O, and CO_2. In this temperature interval, CO_2 formation is best described in terms of CH(a) oxidation, accompanied by water formation, i.e., there is HREELS evidence for O(a) and CH(a) but not CO(a). HCl is formed by abstraction of H from CH_2(a) or CH(a). Methylene may also react with oxygen to form CH(a) and OH(a), the latter promptly forming water. As shown in Figure 17 (panesl E, F, and I), when O(a) increases, the intensities of the 360 K peaks for H_2O and CO_2 increase, but the H_2 peak due to CH(a) dehydrogenation decreases and disappears for O(a) $\geq$ 0.12 ML. We conclude that for a saturation does of $ClCH_2I$ coadsorbed with O(a) $\geq$ 0.12 ML, CCH(a), but not CH(a), exists above 400 K. In the absence of O(a), CCH(a) does not form at 370 K. Thus, O(a) lowers the activation barrier for CCH(a) formation, probably by scavenging H atoms and, in so doing, promotes the reaction to form the thermodynamically favored CCH(a).[74]

By 500 K, XPS and HREELS indicate only Cl(a) and I(a); all hydrocarbon species and O(a) have disappeared. Between 400 and 500 K CO_2 (425 K), H_2O (410 K), HCl (460 K), and

(87) Columbia, M. R.; Crabtree, A. M.; Thiel, P. A. *J. Am. Chem. Soc.* **1992**, *114*, 1231. Avery, N. R. *Appl. Surf. Sci.* **1982**, *11/12*, 774.
(88) Sexton, B. A. *Surf. Sci.* **1981**, *102*, 271. Akhter, S. A.; White, J. M. *Surf. Sci.* **1986**, *167*, 101.
(89) Matsushima, T. *Surf. Sci.* **1982**, *123*, L663.
(90) Hatch, S.; Zhu, X.-Y.; White, J. M.; Campion, A. *J. Phys. Chem.* **1991**, *95*, 1759.

CO (445 K) desorb. The CO_2 peak at 425 K and H_2O at 410 K only appear for O(a) ≥ 0.12 ML, i.e., under conditions where no CH(a) exists and where CCH(a) is the only identifiable surface hydrocarbon species above 400 K. Clearly, CH(a) is more readily oxidized than CCH(a). Significantly, and unlike the oxidation of CH_2(a) (305 K) and CH(a) (360 K), the oxidation of CCH(a) does not lead to coincidental release of H_2O and CO_2. Rather, and reproducibly, CO_2 evolution trails H_2O by about 15 K (~3 s). Assuming C−H bond cleavage determines the rate of H_2O evolution, i.e., H(a) diffuses rapidly, then a delay in the evolution of CO_2 is understandable on the basis that it is relatively difficult to oxidize the resulting C_2, or larger C clusters, i.e., oxidative cleaning of carbon on Pt requires temperatures exceeding 1000 K.

Above 400 K, the following multistep reactions are, thus, inferred:

$$2CCH(a) + O(a) \rightarrow H_2O(g) + 2C_2(a) \text{ at } 410 \text{ K}$$

$$C_2(a) + 4O(a) \rightarrow 2CO_2(g) \text{ at } 425 \text{ K}$$

$$C_2(a) + 2O(a) \rightarrow 2CO(a) \text{ around } 425 \text{ K}$$

$$CO(a) \rightarrow CO(g) \; 445 \text{ K}$$

$$xCCH(a) + xCl(a) \rightarrow xHCl(g) + C_{2x}(a) \text{ at } 460 \text{ K}$$

Because the initial oxygen is all consumed and desorbed at lower temperatures, the last of these reactions removes the final amounts of H. In the absence of initial O(a), the last H is removed as H_2 (Figure 5). The small CO peak at 445 K, even though not detected by HREELS, is probably desorption limited because CO adsorbed on I-covered Pt(111) desorbs at this temperature.[6] In the same regime, 415−440 K, desorption-limited CO was observed from oxidation of C_2H_2,[91] C_2H_4[92] and CH_2N_2[28] on Pt(111).

We now compare the oxidation of $ClCH_2I$ and CH_2N_2.[28] For a saturation dose of CH_2N_2 on 0.21 ML O(a), TPD showed three peaks, 185, 235, and 330 K, for H_2O, a peak at 330 K with a shoulder at 260 K for CO_2 and a peak at 465 K for CO. No CH_2O desorbed. The shoulder at 260 K for CO_2 was attributed to oxidation of CO(a) adsorbed from background. For C_2H_2[91] and C_2H_4,[92] the results were the same. Berlowitz et al.[28] thus concluded that the oxidation of CH_2N_2, C_2H_2, and C_2H_4 on Pt(111) proceeds via the same rate-controlling intermediate-(s) and suggested that either C_2H_x(a) (which, for CH_2N_2, results from the recombination of CH_2(a) before oxidation occurs) or CH(a) was involved. The intensity of the H_2O peak at 185 K was almost the same as at 330 K[28] but was not observed in other laboratories[51,93] when C_2H_4 was oxidized. Because a 185 K peak is normally produced when H(a) and O(a) are present at low temperatures,[94] this peak for CH_2N_2 oxidation may point toward a high background of H_2.[28]

Keeping this difference in mind, we turn to similarities. First, the H_2O peak at 235 K from CH_2N_2 can be correlated to that at 215 K from $ClCH_2I$. The H atoms for this H_2O peak come from dehydrogenation of CH_2(a). Second, the broad H_2O and CO_2 peak at 330 K from CH_2N_2 (which split under certain conditions) correlates with the H_2O and CO_2 peaks at 305 and 360 K from $ClCH_2I$. The 330 K peak for H_2O and CO_2 from CH_2N_2 could result from the oxidation of CH(a) and/or CH_2(a) via an $-O-CH_2-$(a) intermediate like the one we have proposed (note that the evolution of CH_4 at 330 K indicates the existence of CH_2(a)[28]). We suggest that, in the absence of adsorbed halogens, the dehydrogenation and further oxidation of $-O-CH_2-$(a) overwhelms CH_2O desorption. Because the CH_2(a)/O(a) ratio for the CH_2N_2 case is relatively high, there is no O(a) left at high temperature with which to oxidize CCH-(a). Thus, no CO_2 and H_2O evolves above 400 K. There is a third similarity: a small CO peak desorbs around 450 K.

Before closing this section, we comment briefly on the oxidation of $ClCH_2I$ from the environmental point of view. Ideally, the oxidative destruction of halogenated hydrocarbons should lead exclusively to CO_2, H_2O, and HX. The formation of CH_2Cl_2 indicates that on Pt(111) C−Cl bond formation can compete with C−O bond formation and lead to small amounts of undesirable products unless a huge excess of oxygen is used.

4.4. Effect of Halogens on CH_2 Reactions. It is well-known that halogens influence catalyst selectivity. For example, traces of chlorinated hydrocarbons are typically added to the reactant feed of oxygen and ethylene in order to improve the selectivity of Ag/α-Al_2O_3 catalysts for ethylene oxide.[95] Again, while unpromoted Pd is a catalyst for the complete combustion of methane to CO_2 and H_2O,[96] selectivity for partial oxidation of methane to CH_2O and CO occurs in the presence of halogenated hydrocarbons.[97,98] As here, adsorbed halogen atoms, produced by dissociation, are key[95,99] and exert their influence through both geometric and electronic effects. For example, the Cl atoms on Ag(110) block the dissociative adsorption of O_2 (geometric effect) and enhance the adsorption of C_2H_4 by creating $Ag^{\delta+}$ sites (electronic effect).[95]

Following these results, we suppose that the absence of CH_2O formation in the diazomethane−oxygen−Pt(111) system,[28] and its presence in our work for chloroiodomethane−oxygen−Pt(111) indicates a key promotion role for the halogens. The promotion mechanism for CH_2O formation by Cl(a) and I(a) remains to be established, and our observations may motivate studies of how preadsorbed halogens alter the surface electronic structure of Pt(111) and how they influence the adsorption (including coadsorption with oxygen) and reaction of relevant species, e.g., CH_2O, CH_3OH, CO, H_2, and CH_2.

While Cl(a) and I(a) have a significant promotion effect on CH_2O formation, they have little influence on the dehydrogenation and hydrogenation of CH_2(a) because, as noted above, CH_4 formation and desorption is comparable for CH_2N_2 and $ClCH_2I$. To account for our observations, we propose Chart 5 (where Cl(a) and I(a) are assumed to possess negative charge and occupy a threefold site,[100,101] whereas both $[-OCH_2-]$ and CH_2 are described using van der Waals radii). Note that there is no direct experimental evidence for the proposed intermediate, $[-OCH_2-]$. However, it is reasonable and useful for illustrative purposes. Within this framework, its desorption must be competitive with dehydrogenation of $[-OCH_2-]$ if CH_2O(g) is to appear. Since dehydrogenation of CH_2O on clean Pt(111) occurs at 105 K,[156] our data suggests that adsorbed halogens suppress the activity of this process. We assume little or no

(91) Megiris, C. E.; Berlowitz, P.; Butt, J. B.; Kung, H. H. *Surf. Sci.* **1985**, *159*, 184.
(92) Berlowitz, P.; Megiris, C. E.; Butt, J. B.; Kung, H. H. *Langmuir* **1985**, *1*, 206.
(93) Steininger, H.; Ibach, H.; Lehwald, S. *Surf. Sci.* **1982**, *117*, 685.
(94) Ogle, K. M.; White, J. M. *Surf. Sci.* **1984**, *139*, 43.
(95) Campbell, C. T.; Paffett, M. T. *Appl. Surf. Sci.* **1984**, *19*, 28; and the references therein.
(96) Anderson, R. B.; Stein, K. C.; Freeman, J. J.; Hofer, L. J. E. *Ind. Eng. Chem.* **1961**, *53*, 809.
(97) Cullis, C. F.; Keene, D. E.; Trimm, D. L. *J. Catal.* **1970**, *19*, 378.
(98) Mann, R. S.; Dosi, M. K. *J. Chem. Technol. Biotechnol.* **1979**, *29*, 467.
(99) Wang, Y.-N.; Marcos, J. A.; Simmons, G. W.; Klier, K. *J. Phys. Chem.* **1990**, *94*, 7597.
(100) Jo, S. K.; White, J. M. *Surf. Sci.* **1992**, *261*, 111.
(101) Dowben, P. A. *CRC Crit. Rev. Solid State Mater. Sci.* **1987**, *13*, 191.

Chart 5

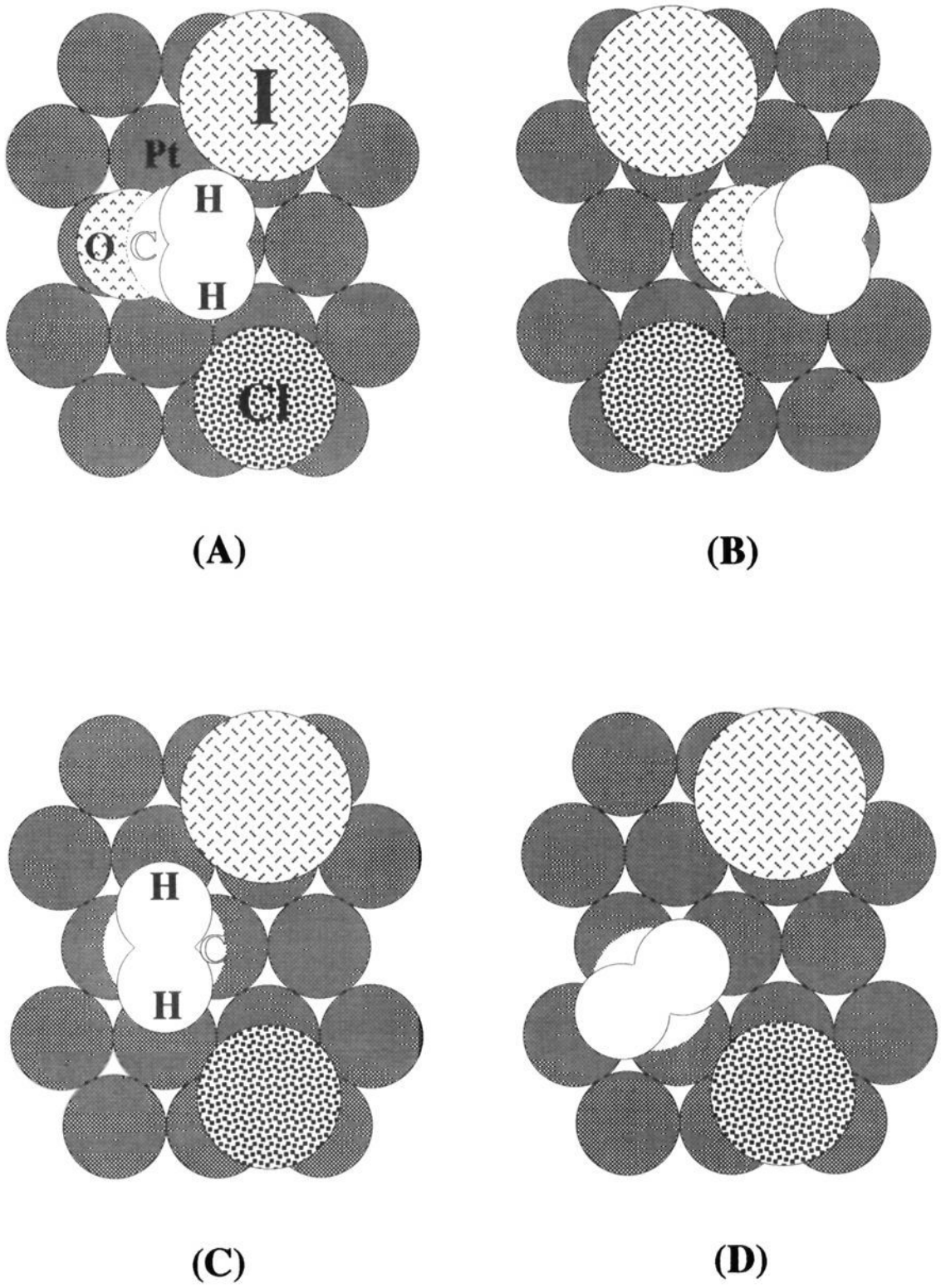

(A) **(B)** **(C)** **(D)**

diffusion for $[-OCH_2-]$ below 280 K. For a structure like Chart 5A, those Pt atoms adjacent to the C−H bonds are occupied by Cl(a) and I(a) and, thus, are strongly modified, i.e., we assume short-range effects dominate.[95] In this case, the C−H bond cleavage is inhibited because either the nearest Pt atoms are passivated so that the effective activation energy for cleavage of the C−H bonds in $[-OCH_2-]$ is high or they are thermodynamically less favorable (on energetic and/or steric grounds) sites for occupation by H atoms. Therefore, desorption of CH_2O becomes kinetically competitive with dehydrogenation. Alternatively, in Chart 5B, Cl(a) and I(a) are placed next to the O atom in $[-OCH_2-]$ and the Pt atoms adjacent to the C−H bonds are not strongly modified. In this case, the C−H bonds break readily making desorption of CH_2O less competitive. Above 280 K, the diffusion of $[-OCH_2-]$ may become significant; if so, the geometry of Chart 5A can be easily converted to that of Chart 5B and lead to the thermodynamically favored products, CO_2 and H_2O, at the expense of CH_2O.

Two intuitively plausible bonding geometries for $CH_2(a)$ are shown in Chart 5 (parts C and D). Here, we assume that Cl(a) and I(a), formed from $ClCH_2I$ dissociation, are not far apart (which is very likely the case because desorption of atomic I and Cl from Pt(111) does not occur until about 800 K so diffusion around 200 K would be slow). In both parts, $CH_2(a)$ can dissociate easily to form CH(a) and H(a), provided the electronic effects of Cl(a) or I(a) are not strongly inhibitory. In the absence of coadsorbed halogens, e.g., CH_2N_2, C_2H_4 forms indicating that $CH_2(a)$ is activated and can recombine, even below 200 K.[28] Thus, short range mobility/reorientation between the geometry of 2C and 2D is plausible. The pairing of $CH_2(a)$ requires, however, longer-range diffusion which, in the presence of Cl(a) and I(a), may be sterically inhibited, accounting for the absence of ethylene in our case.

5. Conclusions

At or below 100 K, $ClCH_2I$ adsorbs molecularly on Pt(111). In subsequent TPD, the physisorbed layers desorb intact at 160 K. In the first monolayer, however, both parent desorption and irreversible dissociation takes place. The fraction depends strongly on the initial coverage; dissociation is exclusive for low doses. For doses that exceed 50% of the first layer, there is parent desorption with peaks at 175 and 233 K. Dissociation begins by breaking the C−I bond (onset at ~150 K), followed by the C−Cl bond (onset at ~170 K), and C−H bonds (onset at ~180 K). The resulting intermediate products include adsorbed I, Cl, CH_2Cl, CH_2, and CH. Complete decomposition of $ClCH_2I$ to form $H_2(g)$, HCl(g), I(a), and $C_x(a)$ dominates for low $ClCH_2I$ coverages. At high coverages, reactions forming

CH_4 and CH_3Cl become important. The estimated first layer coverage is 0.18 ML (molecules of $ClCH_2I$ per Pt). Of this, 28% (0.05 ML) desorbs molecularly, and 72% (0.13 ML) undergoes dissociation and yields 0.109 ML HCl, 0.007 ML CH_4, 0.019 ML CH_3Cl, 0.065 ML of atomic H (desorbing as H_2 after background subtraction of 0.03 ML), and 0.102 ML carbon. The hydrogenation of $CH_2Cl(a)$, to form CH_3Cl, by background H(a) starts at 150 K and peaks at 190 K, while that by H atoms supplied from $CH_2(a)$ dehydrogenation starts at about 180 K and peaks at 210 K. The hydrogenation to CH_3Cl and the dissociation to Cl(a) and $CH_2(a)$ of $CH_2Cl(a)$ are kinetically competitive. The hydrogenation of $CH_2(a)$ to form CH_4 by background H(a) starts at 170 K, while the self-hydrogenation of $CH_2(a)$ to CH_4 starts at about 180 K and peaks at 220 K. HCl and H_2 formation and desorption are rapid at 220 K. While the dissociation of C−I and C−Cl bonds is complete and most of the resulting $CH_2(a)$ fragments react below 260 K, a small fraction of $CH_2(a)$ is stable up to 360 K where it undergoes both self-hydrogenation and reaction with Cl(a) to form gaseous CH_4 and HCl and surface CH. The reaction of Cl(a) with CH(a) to form HCl(g) and CCH(a) occurs at 415 K. All the remaining CH(a) reacts at 520 K to release H_2(g) and form C_x(a) and CCH(a). The decomposition of CCH(a) to form H_2 and more C_x(a) occurs between 600 and 700 K. Surface iodine desorbs atomically between 800 and 900 K. A comparison of our HREELS data with those obtained from C_2H_4 and C_2H_3I, where ethylidyne is involved, suggests that CCH(a) is formed when ethylidyne begins to decompose.

The influence of coadsorbed D atoms is noted in several ways; D(a) (1) lowers the heat of adsorption of $ClCH_2I$; (2) decreases the fraction of the first layer which dissociates; (3) suppresses, for those $ClCH_2I$ admolecules undergoing dissociation, complete decomposition leading to C_x(a); and (4) promotes the reaction channels to methane and methyl chloride. The reaction between dissociated $ClCH_2I$ and D produces not only deuterated methane (CH_3D and CH_2D_2) and methyl chloride (CH_2DCl) but also H−D exchanged methane (CHD_3 and CD_4). Interestingly, no H−D exchanged methyl chloride (i.e., CHD_2Cl and CD_3Cl) was found. The D/H ratio in methane and methyl chloride increases with the preadsorbed D coverage.

Coadsorbed O atoms influence the adsorption and reaction of $ClCH_2I$ in the following ways: (1) increase the heat of adsorption of $ClCH_2I$; (2) suppress parent dissociation slightly; and (3) decrease the yield of the CH-containing reaction products. With 0.25 ML O(a), two kinds of chemisorbed $ClCH_2I$ are evidenced—bound to Pt that is or is not perturbed by O(a). The unperturbed sites lead to CH_4, CH_3Cl, HCl, and H_2O desorption below 250 K. The perturbed sites lead to desorption of oxygenated and chlorinated products above 250 K, e.g., H_2O, CO_2, CO, CH_2O, HCl, and CH_2Cl_2. CH_2O forms below 320 K through the reaction of O(a) with CH_2 and/or CH_2Cl fragments; the proposed intermediate is $-O-CH_2-$(a). CH_2Cl_2 results from the chlorination, between 250 and 320 K, of CH_2Cl fragments. The oxidation of CH_2 and/or CH_2Cl to form H_2O and CO_2 occurs at 305 K; $-O-CH_2-$ and $-O-CH-O-$ are proposed as key intermediates. The oxidation of CH(a) to H_2O and CO_2, and of CCH(a) to CO, occurs between 320 and 400 K and between 400 and 450 K, respectively. When the coverage of coadsorbed O(a) is higher than 0.19 ML, some Cl(a) remains on the surface up to 800 K where it desorbs atomically. That CH_2O desorbs in this study, but not when diazomethane is used,[28] points out the importance of halogens as catalytic promoters that improve the partial oxidation selectivity of transition metals.

Acknowledgment. This work was supported in part by the U.S. Army Research Office, by the Exxon Education Foundation and by the U.S. Department of Energy, Office of Basic Sciences.

JA941981G